Aus dem Max-Delbrück-Centrum
für Moleculare Medizin Berlin-Buch

DISSERTATION

Roles of E-NTPDase1 and 5'-eNT in the Regulation of Microglial Phagocytosis

zur Erlangung des akademischen Grades

Doctor of Philosophy (Ph.D)

im Rahmes des
International Graduate Program Medical Neurosciences

vorgelegt der Medizinischen Fakultät
Charité - Universitätsmedizin Berlin

von

LARISA BULAVINA

aus Simferopol, Ukraine

Gutachter/in:

1. Prof. Dr. H. Kettenmann
2. Prof. Dr. rer. nat. U.-K. Hanisch
3. Prof. Dr. B. Finsen

Datum der Promotion: 23.06.2013

Contents

List of Figures

List of Tables

List of Abbreviations

2-AG	2-Arachydonoyl Glycerate
5'-eNT	Ecto-5'-nucleotidase, also known as CD73
ACP	Acid Phosphatase
ACSF	Artificial Cerebrospinal Fluid
AD	Alzheimer Disease
ADP	adenosine 5'-⟨tetrahydrogen diphosphate⟩
ALP	Alkaline Phosphatase
ALS	Amyotrophic Lateral Sclerosis
AMP	adenosine 5'-⟨tetrahydrogen monophosphate⟩
ATP	adenosine 5'-⟨tetrahydrogen triphosphate⟩
BBB	Brain-Blood-Barrier
BCA	Bicinchoninic Acid
CD39	Ecto-nucleoside triphosphate diphosphohydrolase-1, E-NTPDase1
CD73	Ecto-5'-nucleotidase
CNS	Central Nervous System
COX-2	Cyclooxygenase-2, also known as Prostaglandin-endoperoxide synthase 2

CX3CR1	CX3C chemokine receptor 1, also known as fractalkine receptor or G-protein coupled receptor 13 (GPR13)
DAB	Diaminobenzidine
DAMP	Danger-Associated Molecular Patterns
DAPI	4',6-Diamidin-2-phenylindol
ddH_2O	Distilled Water
DMEM	Dulbecco's Modified Eagle's Medium
DMSO	Dimethylsulfoxide
DNA	Deoxyribonucleic Acid
dNTP	Deoxyribonucleotide Triphosphate
E-NPP	Ectonucleotide pyrophosphatase/phosphodiesterase
E-NTPDase1	Ecto-nucleoside triphosphate diphosphohydrolase-1, also known as CD39
eGFP	Enhanced Green Fluorescence Protein
ENT	Equilibrative Nucleoside Transporters
FCS	Fetal Calf Serum
HBSS	Hank's Balanced Salt Solution
HPLC	High-Performance Liquid Chromatography
IL-1β, -6, -8,...	Interleukin-1β, -6, -8, ...
KA	Kainic Acid
LPS	Lipopolysaccharide
M-CSF	Macrophage Colony-Stimulating Factor
MCAO	Middle Cerebral Artery Occlusion
MRF-1	Microglial Response Factor-1

MS	Multiple Sclerosis
NECA	1-(6-amino-9H-purin-9-yl)-1-deoxy-*N*-ethyl-β-D-ribofuranuronamide, C_{12}-H_{16}-N_6-O_4
NGF	Nerve Growth Factor
NGS	Normal Goat Serum
NO	Nitric Oxide
PBS	Phophate-Buffered Saline
PCD	Programmed Cell Death
PCR	Protein Chain Reaction
PD	Parkinson Disease
PET	Positron Emitted Tomography
PGF_2	Prostaglandin F_2
Pi	Inorganic Phosphate, HPO_4^{2-}
PMA	phorbol 12-myristate 13-acetate
PPADS	pyridoxal-5'-phosphate-6-azophenyl-2,4-disulfonate
PPi	Pyrophosphate, $P_2O_7^{4-}$
rCBF	Regional Cerebral Blood Flow
ROI	Reactive Oxygen Intermediates
TLR	Toll-like Receptor
TNAP	Tissue Non-Specific Form of Alkaline Phosphatase
TNF-α	Tumor Necrosis Factor α
UDP	uridine 5'-⟨trihydrogen diphosphate⟩
UTP	uridine 5'-⟨trihydrogen triphosphate⟩
WT	Wild Type
YG	Fluoresbrite Yellow Green

CHAPTER 1

Introduction

1.1. Microglia: definition, origin and function

Microglial cells are the major representatives of innate immune system cells in the brain and perform the role of brain macrophages. As such, microglia is capable to recognize and eliminate foreign antigens, amyloid plaques, damaged and apoptotic neurons, even without a prior exposition to the antigen (Ransohoff and Perry, 2009).

The first reference to microglial cells come from the work of the Spanish doctor Pío del Río Hortega (1882-1945) (Fig. 1.1). In 1932, he described microglia as cells of mesodermal origin that enter the brain during early development and exhibit ameboid morphology (Del Río Hortega, 1932). Later in development, microglia appeared to be evenly distributed throughout brain parenchyma and possessed a branched, ramified phenotype. Del Río Hortega described as well the transition of resting ramified microglia into the activated ameboid microglia (similar to those of early development) after a pathological event. He observed that activated microglia was able to migrate, proliferate and phagocytose. Despite the abundant investigations done in microglia since then, the validity of these very first observations of Del Río Hortega remains almost intact.

However, the origin of microglia remains even now a debate issues. It

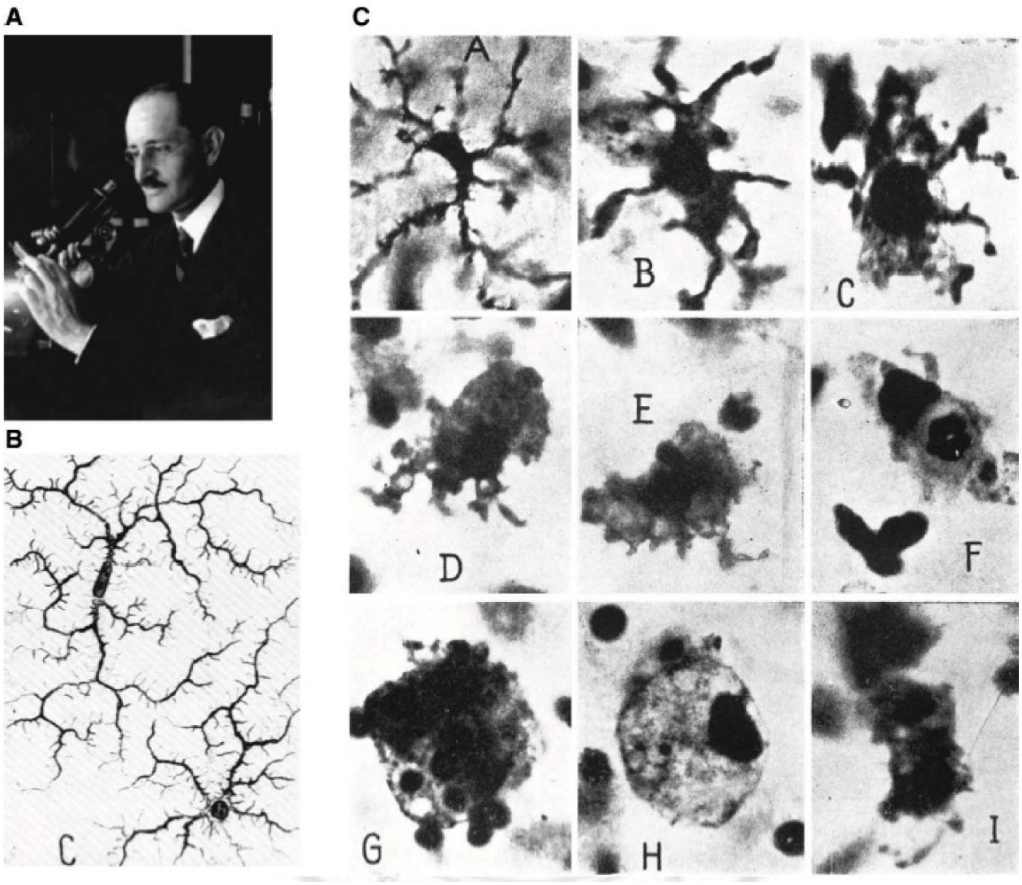

Figure 1.1 – Work of Del Río Hortega.
A. Pío del Río Hortega, Portillo (Valladolid), Spain, 1882 - Buenos Aires, Argentina, 1945 in his laboratory in 1924. **B.** Drawings of ramified microglial cells by Del Río Hortega **C.** Original pictures of Del Río Hortega showing the stages of microglia activation during the phagocytic activity. Microglia was stained with silver carbonate impregnation method. Each picture shows a distinct time point after enthorinal cortex lesion. Modified from Kettenmann et al., 2011.

is generally accepted nowadays that microglial cells originate from mesenchymal stem that derived from blood monocytes, which in turn proceeded from bone marrow. Monocytes enter the brain in early post-natal development and differentiate into brain-specific macrophages. Later studies have found that microglial progenitors are already present in the developing brain at birth (Ginhoux et al., 2010). Here a transgenic mouse line expressing the fractalkine receptor CX3CR1 labeled with Green Fluorescence Protein (GFP) was used to assess the developmental stage at which myeloid cells first occurred in the brain. CX3CR1 expression is routinely considered as a marker of early myeloid progenitors (Harrison et al., 1998) and microglia (Liu et al., 2009). This work showed that myeloid cells expressing CX3CR1 were present in the develop-

ing brain and in yolk sac starting from E9.5. These results demonstrate very interestingly that microglia is not only having specialized functions in the central nervous system (CNS) very early in development but also that microglia precursors are already entering into the brain of embryos from the yolk sac at a point that even the precursors of most other types of macrophages are not developed yet.

Despite being the major population of innate immune cells in the brain, microglia cells are not the only immune cells that are capable of infiltrating the central nervous system (Fig. 1.2). The perivascular space, between the endothelial vessel cells and *glia limitans*, accommodates constantly numerous perivascular macrophages and pericytes. The perivascular macrophages are believed to be blood monocytes that have access to the subarachnoid space but do not actually become resident. On the other hand, pericytes invade the brain during the latter stage of vascularisation and surrounds the newly formed capillary sprouts, eventually becoming enclosed with basal lamina. The phenotypic distinction among pericytes, perivascular macrophages and the permanently resident microglial cells is a major concern for immunohistological, cytological and functional studies (Guillemin and Brew, 2004).

Despite all the new knowledge acquired since the work of Del Río Hortega, only in recent times it was possible to elucidate the different functions of resting microglia in a healthy brain tissue. Based on old and new observations, it was known that microglia is capable of endocytosis of debris and apoptotic material in healthy CNS (Ward et al., 1991). With the increasing development in the field of optical imaging, specially after the introduction of the two-photon microscopy, it became possible to observe microglia in the intact brain of living animals. Here the microglia presented itself as a very active cell type with highly motile processes that could scan permanently their environment (Nimmerjahn et al., 2005; Davalos et al., 2005). Interestingly, these processes were found to transiently contact synaptic elements for up to one hour (Wake et al., 2009), which raised the discussion about the contribution of microglia to synaptic plasticity. After these and other recent observations, the microglia can no longer be considered as a "resting" cell but rather the "surveying" cell of central nervous system (Hanisch and Kettenmann, 2007).

Microglial surveyance is possible thanks to the great variability of receptors that microglia express on its surface. The signaling molecules sensed by

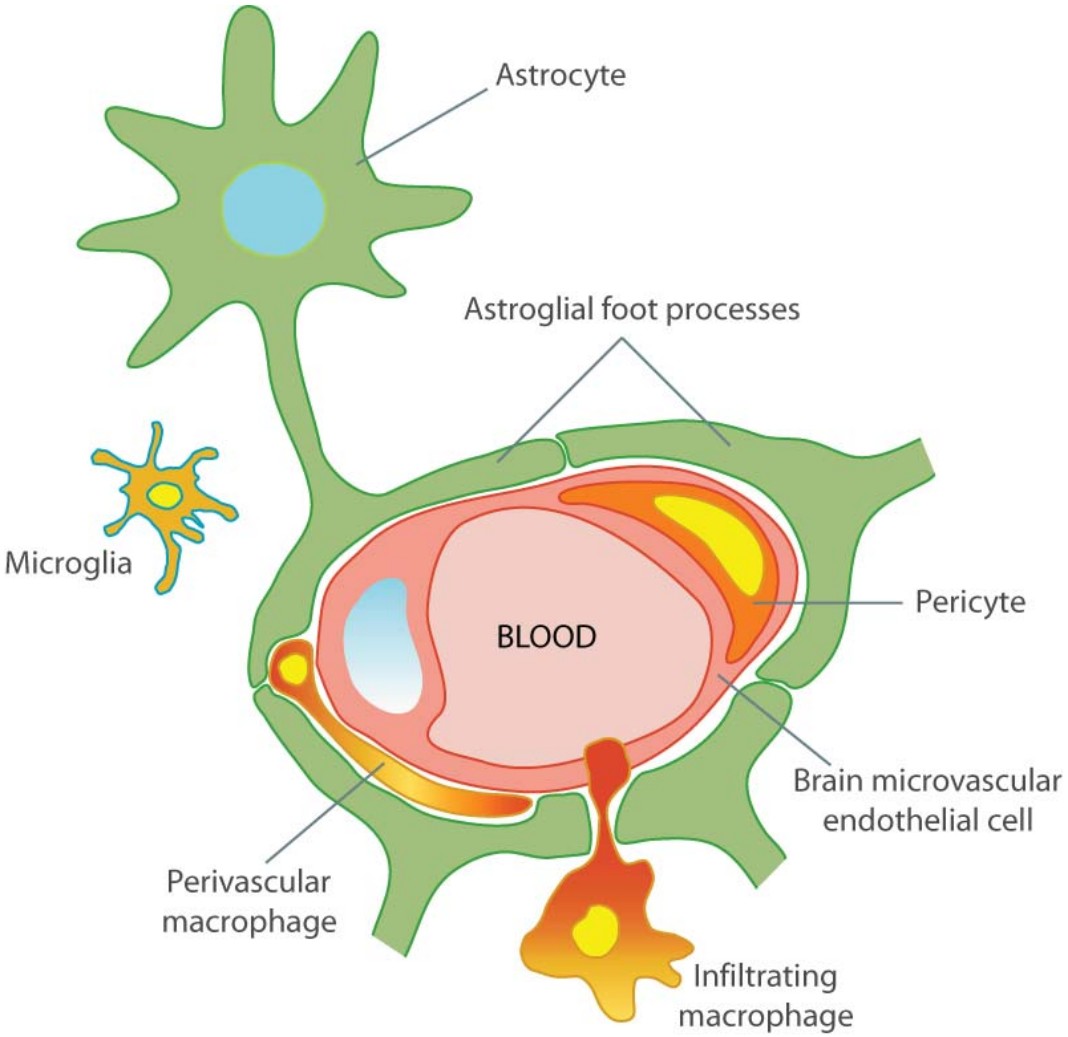

Figure 1.2 – Scheme of the cellular architecture of the brain perivascular area. Pericytes resides in intimate contact with endothelial cell in the brain sharing the basal lamina. Between those and the *glia limitans* formed by the astroglial foot processes, in the so-called perivascular space, there is a constant yet transient presence of macrophages coming from the blood. Under certains conditions, blood macrophages can eventually infiltrate the brain parenchyma. On the other hand, microglia is present in the CNS since a very early developmental stage. Modified from Guillemin and Brew, 2004.

microglia can be assigned to two main groups. The first one include those signals that are constantly present in the parenchyma (*"off" signals*). A second kind of signals are those that appear in the brain after a pathological event (*"on" signals*). Both disrupted *"off"* signaling or sudden appearance of *"on"* signals inevitably causes microglia to go into the one of its activation *"effector"* states (Hanisch and Kettenmann, 2007). Similarly to other macrophagic cells, microglia can exhibit classical or alternative activation states, which are named, respectively, M1 and M2 after the corresponding abbreviations for blood macrophages. In the classical M1 response, microglia react upon bacterial invasion in a dual fashion, by releasing inflammatory mediators and activating phagocytosis (Hanisch et al., 2001; Häusler et al., 2002). On the other hand, during the M2 activation, tasks involving the removal of apoptic cells or myelin debris cause the release of anti-inflammatory factors from the microglia (Magnus et al., 2001; Liu et al., 2005). Classically activated microglia (for instance, upon exposure to LPS or after brain injury) exhibit a characteristic morphology with retracted processes and ameboid soma. However, as already observed by Del Río Hortega, there are many transitional morphological states between the highly branched ramified and the ameboid phenotypes (Fig. 1.1). Once microglial cells are activated, they migrate to the lesion site, where they intensively proliferate, creating an area of reactive microgliosis (Fujita and Kitamura, 1975; Streit et al., 1999).

Early reaction of microglia to the focal lesion of brain parenchyma has been recently studied *in vivo* by means of the two-photon microscopy (Davalos et al., 2005; Haynes et al., 2006; Kim and Dustin, 2006). From these experiments, it is known that a laser lesion on the brain surface causes the polarization of the neighbouring microglia, which sent their processes towards the lesion site, enclosing the local brain damage within minutes. It was further shown that microglia sensed the extracellular ATP (adenosine 5'-⟨tetrahydrogen triphosphate⟩) released from the damaged cells through $P2Y_{12}$ purinergic receptors (Haynes et al., 2006).

Microglia express variety of purinergic receptors, which modulate broad spectrum of functions, such as migration, phagocytosis, proliferation, apoptosis, as well as pro- and anti-inflammatory cytokine release. Koizumi et al. (2007) showed that UDP (uridine 5'-⟨trihydrogen diphosphate⟩), acting via $P2Y_6$ receptors, lead to the increase of microglial phagocytosis *in vitro* as

well as *in vivo*. In contrast, short-term exposure of microglial cells to high concentrations of ATP attenuated microglia phagocytic activity by a $P2Y_7$-receptor mediated mechanism (Fang et al., 2009). In addition to purinergic receptors, microglia express an extent repertory of other kinds of receptors, such as: neurotransmitter receptors for glutamate, GABA, dopamine, acetylcholine and adrenaline; receptors for neurohormones and neuromodulators (bradykinin, histamin, cannabinol, endothelin, angiotensin, somatostatin, etc.); as well as cytokine, chemokine and *Toll-like* (TLR) receptors. Microglia maintain a constant communication with other cells by releasing of pro- and anti-inflammatory cytokines, chemokines, growth factors, proteins and peptides. Microglia can actively induce an acute inflammatory response by producing nitric oxide (NO) and other reactive oxygen species (Kettenmann et al., 2011).

In contrast to the acute inflammation, which refers to the early and transient episodes of microglia activation, in a chronic inflammation the activation of the immune cells persist. Chronic inflammation is considered to be detrimental and it is frequently involved in autoimmune and neurodegenerative diseases, such as multiple sclerosis, Alzheimer or Huntington disease. It is known that microglia play an important role during chronic inflammation as well and it may influence the pathogenesis of neurodegenerative processes (Krabbe et al., 2011).

1.2. Metabolism of extracellular ATP in the CNS

1.2.1 Extracellular ATP as danger signal molecule

ATP is a ubiquitous molecule. In the CNS it is present in the cytoplasm of nerve terminals, astrocytes, and the microglia itself. It is released to the extracellular space in response to a wide variety of signals, including neuronal firing, mechanical stimuli, ischemia or energy deprivation, bacterial endotoxins and cellular distress or damage. ATP acts in these situations as a local signal of damage and may initiate the inflammatory response. The american immunologist Polly Matzinger was the first who proposed that the immune system can recognize and respond to the endogenous substances, released from damaged cells into the extracellular compartment (Matzinger, 2007). Such endogenous

danger signaling molecules, including ATP, are called danger-associated molecular patterns (DAMPs) and fulfill several defined criteria (Di Virgilio, 2005) :

- High intracellular concentrations: 5-10 mM for intracellular ATP, 0.5-1 mM for intracellular UTP.
- Negligible extracellular concentrations under the normal physiological conditions: the extracellular ATP concentration under resting condition is in the 1-10 nM range.
- High mobility in the pericellular aqueous environment (i.e. small hydrophilic molecules): ATP is a small solute (molecular mass 650 Da) bearing from two to four negative charges, depending on the pH and Ca^{2+} and Mg^{2+} concentration, which makes it highly diffusible in the extracellular *aqueous milieu*.
- Released danger molecules bind to their specific receptors and trigger specific immune responses: as of now 15 receptors for extracellular nucleotides have been identified (Di Virgilio, 2005). The widely differing range of nucleotide specificity and affinity makes this receptor family very flexible and efficient in translating information delivered by the ligands.
- Released danger molecules can be quickly removed from extracellular space: in case of ATP, removal from the extracellular space is to large extent performed by two ectoenzymes – CD39 (or E-NTPDase1) and CD73 (or 5'-ectonucleotidase, 5'-eNT). Both enzymes are specifically expressed by microglia and by endothelial cells on the other side of the blood-brain barrier.

1.2.2 Ectonucleotidases regulate P2 and P1 signaling

Purinergic receptors can be divided into two categories depending on the ligand affinity. Extracellular nucleotides, mainly ATP, bind to P2 receptors. On the other hand, P1 receptors are activated by adenosine. Both types of receptors are known to actively participate in numerous physiological processes (Abbracchio et al., 2009). Thus, ATP signaling in the microglia must be tightly coordinated in order to assure a proper function. The regulation of ATP-mediated microglia activation is done through two main mechanisms. First, receptor expression and sensitization are intrinsically fine-tuned by microglia.

Second, ATP concentration at the cell surface and, consequently, the magnitude of purinergic receptor stimulation are object of a strict control. Microglia itself is able to influence the amount of purinergic activation by expressing ectonucleotidases on the cell membrane or secreting them to the extracellular medium, where they are able to hydrolyze the surrounding nucleotides into the corresponding nucleoside and free phosphate (Fig. 1.3).

Ectonucleotidases are involved in multiple aspects of P2 and P1 receptor signaling. Some of these include the termination of P2 receptor activation, protection of susceptible P2 receptors from desensitization, generation of ligands for P2 receptors by hydrolyzing triphosphonucleotides to diphosphonucleotides, as well as production of extracellular adenosine that activates P1 receptors. These enzymes are not only localized in the CNS but they show a broad tissue distribution as well (Kukulski et al., 2005).

The currently characterized ectonucleotidases can be classified into four families (Zimmermann, 2001):

1. Ecto-nucleoside triphosphate diphosphohydrolase (E-NTPDase) family.
2. Ectonucleotide pyrophosphatase/phosphodiesterase (E-NPP) family.
3. Alkaline and acid phosphatases (ALP and ACP).
4. Ecto-5'-nucleotidase (CD73).

In the CNS, E-NTPDase1 (CD39) and 5'-ectonucleotidase (CD73) are expressed by microglia and act by degrading ATP to adenosine. This newly originated adenosine adds to the one coming from the transport through equilibrative nucleoside transporters to create a pericellular purinergic signal (Colgan et al., 2006; Parkinson et al., 2005; Sowa et al., 2009). Extracellular adenosine activates P1 receptors (A_1, A_{2A}, A_{2B} and A_3) to execute specific responses that often are opposite to those mediated by P2-receptor activation (Jacobson and Gao, 2006). In addition, the adenosine levels are also controlled by surrounding cells that incorporate adenosine, which is later on reused for nucleotide resynthesis (Pastor-Anglada et al., 1998).

1.2.3 NTPDase family function and structure

The NTPDase family consists of eight members, that is, NTPDase1–8 (Robson et al., 2006). NTPDase1, -2, -3, and -8 are type II membrane proteins

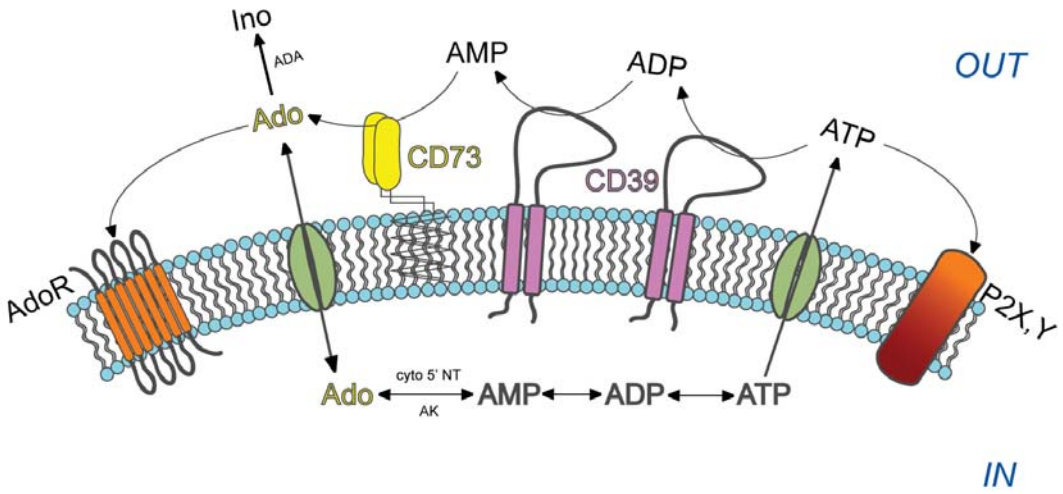

Figure 1.3 – Metabolism of ATP in the extracellular space.
ATP stored in the intracellular compartment is released into the extracellular space, where it can activate P2 receptors (P2X or P2Y) or get hydrolized to adenosine (Ado) by ectonucleotidases CD39 and CD73. Adenosine can activate adenosine receptors (AdoR) or get hydrolized to ionosin (Ino) by adenosindeaminase (ADA). Adenosine inside the cell can be converted to AMP by adenosin kinase (AK). AMP, in turn, can be hydrolized back to adenosine by cytosolic 5'-nucleotidase (cyto 5' NT). Modified from Pexa and Deussen, 2005.

(Fig. 1.4) that efficiently hydrolyze all nucleotides capable of activating P2 receptors, such as adenine and uracil tri- and diphosphonucleosides, as well as other nucleotides without a demonstrated action over P2 receptors. On the other hand, NTPDase4–7 are localized in intracellular organelles and do not participate in the metabolism of extracellular nucleotides (Robson et al., 2006).

The hydrolysis of nucleotides by these enzymes requires the presence of calcium (Ca^{2+}) or magnesium (Mg^{2+}) ions (Kukulski et al., 2005; Zimmermann, 2001). NTPDases show catalytic properties at a wide range of pH, although they exhibit the best activity at pH 7.0–8.5 (Kukulski et al., 2005). Due to differences in ATP and UTP hydrolysis kinetics, individual plasma membrane NTPDases can affect differently the activation of ADP- and UDP-dependent P2 receptors.

In the CNS, three members of this family are known to be expressed: E-NTPDase1, 2 and 3. Expression in the brain of E-NTPDase1 (also called CD39) is restricted to microglial cells and vascular endothelium (Braun et al., 2000), which might indicate that this enzyme could play a major role in the removal of extracellular ATP and ADP in the parenchyma. The kinetic activity for both ATP and ADP to AMP is very fast, which effectively removes

all possible activators of P2X and P2Y purinergic receptors from the extracellular space. However, NTPDase1 exhibits a substantially smaller K_m in comparison to the other members of its family, which allows the hydrolysis of phosphopurines at concentrations at least 3 times lower (Kukulski and Komoszyński, 2003). As consequence, NTPDase1 can most efficiently terminate the P2-receptor mediated signaling or prevent its inactivation (for a review see Kukulski et al., 2011).

E-NTPDase2 is, on the other hand, mostly expressed on astrocytes. Although this enzyme shows a certain ADP hydrolytic activity, its action mechanism consists preferentially on the hydrolysis of ATP to ADP (Robson et al., 2006), with the end effect of ADP accumulation.

The last member of the family, E-NTPDase3, is believed to be expressed in neurons (Belcher et al., 2006). Its kinetic properties lay in between E-NTPDase1 and 2, resulting in the removal of ADP from extracellular space at a slower rate than E-NTPDase1. Interestingly, all plasma membrane NTPDases are able to dephosphorylate UTP, leading to a significant accumulation of UDP, which, in turn, causes the activation of $P2Y_6$ receptors (Kukulski et al., 2011).

1.2.4 Ecto-5'-Nucleotidase function and structure

The ecto-5'-nucleotidase (also known as CD73, Figure 3.9) is a glycoprotein consisting of two 60-74 kDa subunits associated through non-covalent bonds (Zimmermann, 1992). This enzyme binds Zn^{2+} and other divalent cations, required for the enzymatic activity, and has a broad specificity towards nucleoside monophosphates with a K_m in the range of 3-50 μM (Zimmermann, 1992). In the brain tissue, it is abundant on microglia but it can be found in vasculature, neurons and astrocytes as well (Yegutkin, 2008; Zimmermann, 1992). Interestingly, a recent study disproved the presence of CD73 from blood vessels of mouse brain (Langer et al., 2008). The main function of this enzyme resides in the generation of extracellular adenosine from AMP.

The ecto-5'-nucleotidase shows affinity to any kind of nucleoside monophosphate, however, nucleoside tri- and diphosphates are not able to be hydrolyzed. Furthermore, ATP and specially ADP, which are the most common substrates of NTPDases, are potent inhibitors of this enzyme (Zimmermann, 1992).

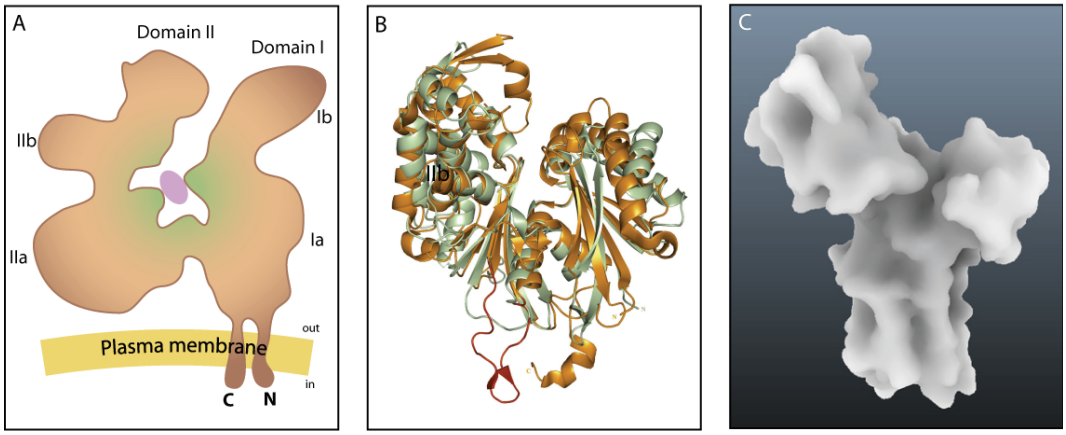

Figure 1.4 – Topology of a surface-located NTPDase with two transmembrane domains.
A. Schematic representation of the CD39 structure. Modified from Robson et al., 2006. A comparison of the conserved secondary structure reveals duplicate conservation of two major domains related to subdomains Ia and IIa of actin, and other members of the actin/HSP70/sugar kinase superfamily. In contrast to the other members of the superfamily, surface-located NTPDases are anchored to the plasma membrane by terminal hydrophobic domains. The figure takes into account the close distance of the N-and C-terminus of actin at domain I and the binding of ATP (*red*) in the cleft between domains I and II. These two domains are expected to undergo conformational changes involving movement relative to each other. **B.** Crystal structure of a Legionella pneumophila NTPDase, a structural and functional homolog of the eukaryotic NTPDases (Vivian et al., 2010). **C.** 3D reconstruction of a Legionella pneumophila NTPDase using Molecular Maya plugin for Autodesk Maya™ 2011 (PDB ID 3AAP © *L. Bulavina*).

1.2.5 Other ectonucleotidases expressed in the CNS

Alkaline phosphatases

Most of the members of the mammalian alkaline phosphatase (ALP) family are composed of two covalently bound identical subunits. The enzyme is attached to the plasma membrane via a glycosylphosphatidylinositol (also known as GPI anchor) at the C-terminus (Millán, 2006). Alkaline phosphatases are able to degrade nucleoside 5'-tri-, -di-, and -monophosphates and a large variety of other organic compounds, including proteins (Millán, 2006), releasing pyrophosphates ($P_2O_7^{4-}$, PPi) that are afterwards hydrolyzed to inorganic phosphate (HPO_4^{2-}, Pi). These enzymes are, furthermore, capable of directly causing the hydrolysis of the extracellular ATP producing the P1 receptor agonist adenosine. The highest enzymatic activity is reached in the high alkaline range, however they can also hydrolyze ATP very efficiently at a pH of 7.4. The tissue non-specific form of alkaline phosphatase (TNAP) has been located to the endothelium of brain capillaries. Additional electron-microscopic studies

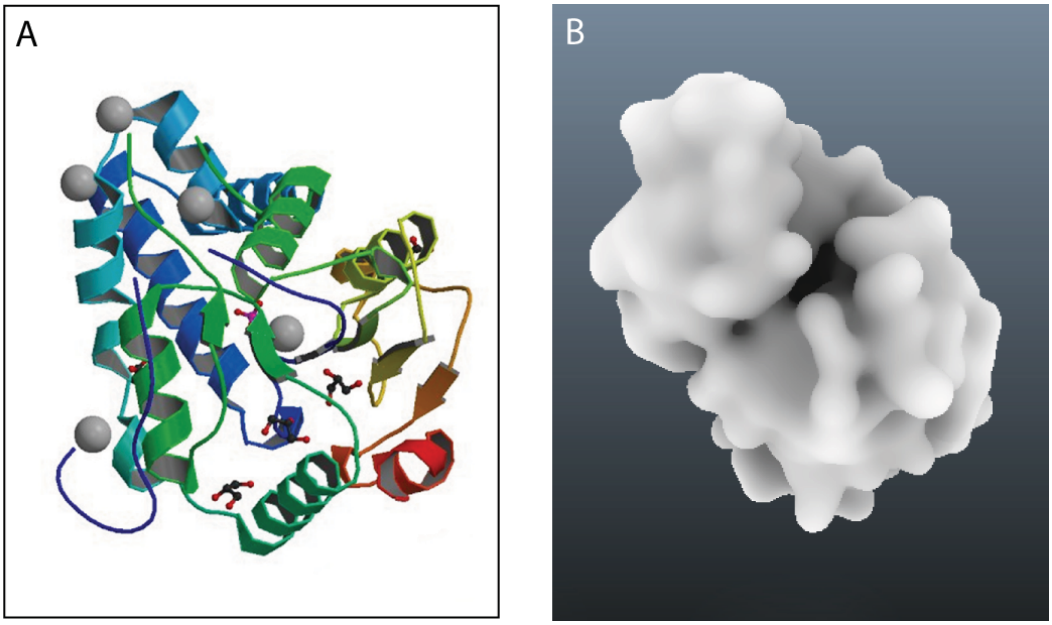

Figure 1.5 – Tridimensional structure of CD73.
A. Crystal Structure of the periplasmic Haemophilus influenzae NAD nucleotidase, a structural and functional homologue of the eukaryotic CD73 (Garavaglia et al., 2012). **B.** 3D reconstruction of the above mentioned structure using Molecular Maya plugin for Autodesk Maya™ 2011 (PDB ID 3ZU0 © *L. Bulavina*).

suggest that this enzyme is also present in astrocyte endfeet facing the vascular basement membrane, gap junctions and immature oligodendrocytes (Vorbrodt et al., 1982, 1986; Mori and Nagano, 1985; Chilingaryan et al., 2006). It is believed that TNAP might support ecto-5'-nucleotidase action in conditions that require more effective AMP hydrolysis and adenosine production (Millán, 2006).

Nucleotide Pyrophosphotases / Diphosphodiesterases (E-NPPase family)

Three members of the E-NPPase family (NPP1, -2 and -3) are specialized in the hydrolysis of pyrophosphate bonds in nucleotides (Stefan et al., 2005). In addition to ATP and ADP, these enzymes can use extracellular dinucleoside polyphosphates as substrates as well (Vollmayer et al., 2003). For optimal activity, NPP1, 2 and 3 require alkaline pH and the presence of divalent ions, that is, Zn^{2+} and Mg^{2+} (Gijsbers et al., 2001). NPP1 and NPP3 are both anchored to the plasma membrane and only NPP2 is released to the extracellular medium. It has been found the presence of these three diphosphodiesterases in the brain at different extent (Stefan et al., 2005). However, microglia and blood vessels appear to be the predominant structures expressing NPPs. The

function of these enzymes here seems to be the termination of the P2 receptor signaling by hydrolysing ATP to AMP and pyrophosphate (PPi), with K_m values of approximately 10 µM (Kukulski et al., 2011).

1.3. Purinergic modulation of microglia function

Purinergic activation can be mediated through two kind of membrane receptors, P1 and P2. Whereas adenosine selectively binds to P1 metabotropic receptors (A_1, A_{2A}, A_{2B} and A_3), extracellular tri- and dinucleotides act through P2 purinergic receptors. Seven ionotropic ($P2X_{1\text{-}7}$) and eight metabotropic receptors ($P2Y_1$, $P2Y_2$, $P2Y_4$, $P2Y_6$, $P2Y_{11\text{–}14}$) have been discovered. The intrinsic channel of the P2X receptors allows a non-selective flow of ions after the conformational switch produced upon ATP binding. P2Y receptors, on the other hand, couple the binding of either purine or pyrimidine nucleotides or sugar nucleotides subtype-dependently to intracellular second-messenger systems through heteromeric G-proteins (Fig. 1.6).

1.3.1 Regulation of the function of microglia by adenosine

Activated microglia play a key role in chemotaxis, phagocytosis, neuropathic pain as well as pro- and anti-inflammatory events in the CNS. These effects are believed to be modulated by the specific action of the different purinergic receptors (Fig. 1.6). Although it has been shown the expression of A_1 receptors, A_{2A} receptors and A_3 receptors in microglia, there is no evidence that they contain A_{2B} receptors as well (Haskó et al., 2005). It seems that the overall activation of these receptors through adenosine modulate both pro- and anti-inflammatory microglial response in the CNS. Unfortunately, the role of A_3 receptor stimulation in regulating microglial function was not determined up to now. Adenosine receptor stimulation can cause, similarly as in astrocytes, microglial apoptosis (Ogata and Schubert, 1996). It is known that, in general, adenosine stimulates the proliferation of naïve microglial cells through a mechanism that involves the simultaneous activation of A_1 receptors and A_{2A} receptors (Gebicke-Haerter et al., 1996). On the other hand, adenosine can also inhibit the proliferation of microglial cells under certain conditions. For example, phorbol 12-myristate 13-acetate (PMA)-stimulated

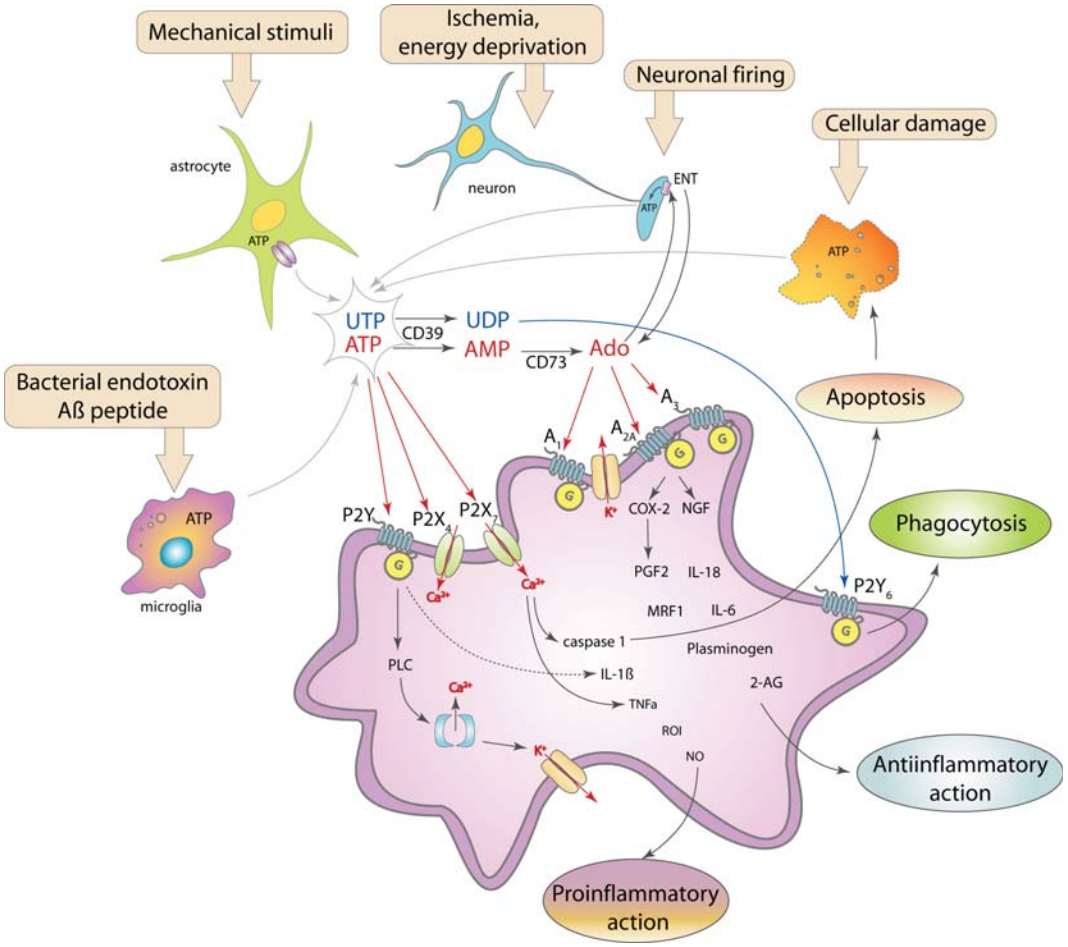

Figure 1.6 – A summary of purinergic pathways involved in microglial response. ATP exerts its action in the microglia mainly through the ionotropic $P2X_7$ and $P2X_4$ receptors as well as through the metabotropic P2Y receptors. Adenosine, on the other hand, activates P1 receptors such as A_1, A_{2A} and A3, which are abundant on the surface of activated microglia. These receptors regulate the proliferation/survival of microglia, COX-2 expression and subsequent secretion of PGF_2 and the production of nerve growth factor (NGF). The activation of P2 receptors results in a elevation of the intracellular Ca^{2+} concentration. P2X receptors are furthermore involved in the expression, posttranslational processing and secretion of various proinflammatory and antiinflammatory mediators (i.e., IL–1β, IL–6, IL–8, TNF-α, reactive oxygen intermediates (ROI), plasminogen, 2-arachydonoyl glycerate (2-AG), and microglial response factor-1 (MRF-1) amongst others). The stimulation of P2Y receptors can moreover produce a hyperpolarisation of the microglia, via an outward K^+ conductance, which inhibits the production of proinflammatory mediators. In addition, $P2Y_7$ receptors may eventually provoke apoptosis by caspase-1 activation. Cellular damage or death produces an increase in the extracellular UTP. Stimulation of $P2Y_6$ by UDP, generated via breakdown of UTP by NTPDase1, leads to a increased phagocytic activity of microglia. Modified from Sperlágh and Illes, 2007.

microglial proliferation is reduced following treatment with an A_1 receptor agonist (Si et al., 1996). In addition, secretory activity of microglia appears to be stimulated by A_{2A} receptors. For example, A_{2A} receptor stimulation upregulates cyclooxygenase 2 (COX-2) and the release of prostaglandins. It is known that prostaglandin E_2 (PGE_2) has an pro-inflammatory effect, which might potentiate the pro-inflammatory effect of A_{2A} receptor stimulation (Fiebich et al., 1996). By contrast, other products of COX-2, such as PGD_2 and 15-deoxy-PGJ_2, have an effect in the resolution of inflammation (Gilroy, 2004), which would indicate that the induction of COX-2 activity by adenosine in microglial cells might be a beneficial, neuroprotective feature.

1.3.2 Regulation of the function of microglia through P2 receptors activation

Nucleotide activation of microglia is believed to be mediated by the receptors $P2X_4$, $P2X_7$ and $P2Y_1$, $P2Y_2$, $P2Y_6$, $P2Y_{12}$, $P2Y_{13}$ and $P2Y_{14}$ (Inoue, 2008). From those, $P2Y_6$ was recently assigned to a promotion of microglial phagocytosis (Koizumi et al., 2007). In this work, neuronal injury caused by kainic acid (KA) produced an increase of extracellular UTP by the KA-evoked neuronal injury and at the same time upregulation of the expression of $P2Y_6$ receptors in microglia. Extracellular UTP is immediately metabolized into UDP *in vivo* and *in vitro* (Kukulski et al., 2011) and this increased concentration of extracellular UDP causes a promotion of the $P2Y_6$ receptor-dependent phagocytosis both *in vivo* and *in vitro* (Koizumi et al., 2007). Interestingly, ATP/ADP is not able to activate efficiently $P2Y_6$ receptors but, on the other hand, UDP cannot act on $P2Y_{12}$ or $P2Y_{13}$ receptors. This indicates that the simultaneous increase of both adenine and uridine nucleotides in the extracellular medium regulate microglial chemotaxic and phagocytic responses in a mutually exclusive but coordinated fashion (Koizumi et al., 2007) (Fig. 1.6).

1.4. Aim of the work

The aim of the present study was to elucidate the roles of CD39 and CD73 enzymes in the regulation of microglial phagocytosis by analysis of the convertion of the extracellular P2 purinoreceptor activators ATP and ADP to AMP and the end production of the P1 activator adenosine from AMP.

To reach this goal, we have developed the methods to assess microglial phagocytic activity and measure the extracellular enzyme activities involved in the reaction cascade catalyzing ATP to adenosine (Fig. 1.3):

$$\text{ATP} \rightleftharpoons \text{ADP} \rightleftharpoons \text{AMP} \rightleftharpoons \text{Adenosine}$$

in living tissue samples from mouse brain.

Using these new technical approach, we aim at answering the following specific questions:

1. What is the overall microglial contribution to removal of extracellular ATP and ADP and to the generation of adenosine from AMP in the brain tissue?
2. What role do CD39 and CD73 enzymes take in the regulation of microglial phagocytic activity during brain development?
3. How does activation of P2 and P1 purinergic receptors affect the phagocytic activity of parenchymal microglia?

Answers to these question may, in turn, provide us with the insights into treatment of Alzheimer disease, multiple sclerosis, amiotrophic lateral sclerosis, prion disease amongst others, where microglial phagocytic activity play an important role in the disease progression.

CHAPTER 2

Materials & Methods

2.1. Materials

2.1.1 Chemicals

Chemical	Company
Adenosine triphosphate (ATP)	Sigma-Aldrich, Munich, Germany
Adenosine diphosphate (ADP)	Sigma-Aldrich, Munich, Germany
Adenosine monophosphate (AMP)	Sigma-Aldrich, Munich, Germany
Aqua-Poly/Mount	Polysciences Europe Gmbh, Eppelhein, Germany
Bovine Serum Albumin (BSA)	Fluka Chemie, Buchs, Switzerland
Chlodronate	Calbiochem, Darmstadt, Germany
Clodronate-filled liposomes	Dr. Nico van Rooijen `http://www.clodronateliposomes.org`
Cytochalasin D	Sigma-Aldrich, Munich, Germany
DePeX mounting medium	VWR International GmbH, Wien, Germany
Diaminobenzidine (DAB)	Sigma-Aldrich, Munich, Germany
Dimethylsulfoxide (DMSO)	Sigma-Aldrich, Munich, Germany
Direct PCR-Tail	PeqLab, Erlangen, Germany

Dulbecco's Modified Eagle Medium (DMEM)	Gibco, Eggenstein, Germany
Ethanol	Roth, Karlsruhe, Germany
Ethidiumbromide	Sigma-Aldrich, Munich, Germany
Fetal Calf Serum (FCS)	Gibco, Eggenstein, Germany
Fetal Bovine Serum (FBS)	Atlanta Biologicals, USA
Fluoresbrite Yellow Green (YG) Carboxylate Microspheres	Polysciences Inc, Warrington, USA
L-Glutamine	Biochrom AG, Berlin, Germany
Hank's Balanced Salt Solution (HBSS)	Biochrom AG, Berlin, Germany
HEPES	Carl Roth, Karlsruhe, Germany
H_2O_2, 30% solution	Carl Roth, Karlsruhe, Germany
Insulin	Gibco, Eggenstein, Germany
Lipopolysaccharide (LPS)	Sigma-Aldrich, Munich, Germany
Methanol	Roth, Karlsruhe, Germany
Narcoren	Bela-Pharm, Vechta, Germany
Normal Goat Serum (NGS)	Sigma-Aldrich, Munich, Germany
Paraformaldehyde	Merck, Darmstadt, Germany
Penicillin/Streptomycin	Biochrom AG, Berlin, Germany
pHRodo E.coli Bioparticles	Invitrogen, Karlsruhe, Germany
Poly-L-Lysine	Sigma-Aldrich, Munich, Germany
Propidium Iodide	Sigma-Aldrich, Munich, Germany
Proteinase K	PeqLab, Erlangen, Germany
Sucrose	Merck, Darmstadt, Germany

TaKaRa Ex Taq Hot Start polymerase	TaKaRa, Madison, USA
Taq polymerase	Invitrogen, Karlsruhe, Germany
Tris-HCl	Roth, Karlsruhe, Germany
Triton X-100	Carl Roth, Karlsruhe, Germany
Trypan blue	Invitrogen, Karlsruhe, Germany
Trypsin	Gibco, Eggenstein, Germany
Tween 20	Merck, Hohenbrunn, Germany
Vitamin C	Sigma-Aldrich, Munich, Germany
β-mercaptoethanol	Invitrogen, Karlsruhe, Germany

Table 2.1 – Chemicals

2.1.2 Buffers and solutions

Buffer / Solution	**Content**
ACSF buffer	134 mM NaCl, 2.5 mM KCl, 1.3 mM $MgCl_2$, 2 mM $CaCl_2$, 1.26 mM K_2HPO_4, 10 mM D-glucose, 26 mM $NaHCO_3$; pH7.4
Block buffer for DAB staining	10% v/v methanol, 10% v/v 30% H_2O_2 in PBS
Cultivation medium for organotypic slices	DMEM supplemented with 25% heat-inactivated FCS, 50 mM Na_2HCO_3, 2% glutamine, 25% HBSS, 1 mg/mL insulin, 2.46 mg/mL glucose, 0.8 mg/mL vitamin C, 100 U/mL penicillin, 100 mg/mL streptomycin, 5 mM Tris
Culture medium for organotypic slices	DMEM supplemented with 10% heat inactivated FBS, 0.2 mM glutamine, 100 U/mL penicillin, 100 mg/mL streptomycin

DEPC water	0.01% (v/v) Diethylpyrocarbonat (DEPC), autoclaved
Dilution Buffer	1:10 (v/v) of permeabilisation buffer in 0.1 M PB; pH 7.4
dNTP	Invitek, Berlin, Germany
Hepes Buffered Solution (HBS) for phagocytosis assay	50 mM HEPES, 135 mM NaCl, 5mM KCl, 1.8 mM $CaCl_2$, 1 mM $MgCl_2$, 5.6 mM D-glucose
L929 conditioned medium	L929 fibroblasts were grown to 80% confluence in a T75 flask, 30 ml fresh DMEM was added, 2 days after medium was harvested, filtered and mixed with 2/3 (v/v) DMEM
PB	100 mM Na_2HPO_4, 100 mM NaH_2PO_4
PBS	137 mM NaCl, 2.7 mM KCl, 4.3 mM Na_2HPO_4, 1.4 mM KH_2PO_4; pH 7.4
TAE buffer	10 mM Tris-Acetate, 1 mM EDTA; pH 8.0
Reaction buffer for orthophosphate determination	20 mM HEPES, 135 mM NaCl, 5 mM KCl, 1.8 mM $CaCl_2$, 1 mM $MgCl_2$, 5.6 mM D-glucose
Permeabilisation buffer	2% (v/v) Triton X-100, 2% BSA, 10% NGS in 0.1 M PB; pH 7.4

Table 2.2 – Buffers and Solutions

2.1.3 Antibodies and fluorescent probes

Probe	Company
Alexa® 633 goat anti rabbit	Invitrogen, Karlsruhe, Germany
Griffonia simplicifolia isolectin B_4	Sigma, Deisenhofen, Germany
Hoechst 33342	Invitrogen, Karlsruhe, Germany
Biotinilated goat anti-rabbit antibody	Abcam, Cambridge, UK
Biotinilated goat anti-rat antibody	Abcam, Cambridge, UK
Monoclonal rat anti-mouse CD11b antibody	Serotec, Düsseldorf, Germany
Polyclonal rabbit anti-mouse Iba1 antibody	Wako Pure Chemicals, Japan
Tomato lectin-conjugated Alexa Fluor®594	BioTez GmbH, Berlin, Germany
4',6-Diamidin-2-phenylindol (DAPI)	Sigma-Aldrich, Munich, Germany

Table 2.3 – Antibodies and fluorescent probes

2.1.4 Primers

Specificity	Sequence
CD39 WT, forward (D3M)	5'ACT GTT TAT ATC CCA AGG AGC TGG CAT AGG 3'
CD39 WT, reverse (MEC8P)	5'GAC AGA CGA GGG AAG AGG AAG G 3'
CD39 KO, forward (D3M)	5'ACT GTT TAT ATC CCA AGG AGC TGG CAT AGG 3'
CD39 KO, reverse (NEOP2)	5'TAC CCG TGA TAT TGC TGA AGA GCT TGG CGG 3'
CD73 WT, forward (SC3)	5'-TGG GAA ATC ATG AAT TTG ATA ACG-3'

CD73 WT, reverse (SC4)	5'-GGT TTC CTT TGA AGT ATA TCC AAC-3'
CD73 KO, forward (NeoRS)	5'- ACA ACA GAC AAT CGG CTG CTC TGA TG -3'
CD73 KO, reverse (NeoRas)	5'- TGC GCG CCT TGA GCC TGG CGA AC -3'

Table 2.4 – Primers

2.1.5 Kits

Description	**Company**
Elite ABC Kit	Vector Lab., Burlingame, CA, USA
BCA total protein assay	Pierce Biotechnology, Rockford, USA
Malachite green phosphate assay Kit	BioAssay Systems, Hayward, USA

Table 2.5 – Kits

2.1.6 Equipment and Devices

Description	Company
Axiovert FS microscope	Zeiss, Oberkochen, Germany
Leica LSM laser scanning confocal microscope	Leica, Wetzlar, Germany
Microplate plate reader Infinite M200	Tecan, Crailsheim, Germany
Vibratome VT 1000 S	Leica, Heidelberg, Germany
Vibratome HM650V	Microm, Walldorf, Germany
Ultrasound processor UP 50H	Dr. Hielscher GmbH, Berlin, Germany
Cryostat Leica CM1950	Leica, Nussloch, Germany

Table 2.6 – Equipment and Devices

2.1.7 Computer Software

Software	Company
Adobe Acrobat 6.0 Professional	Adobe Systems, USA
Adobe Illustrator CS5	Adobe Systems, USA
Adobe Photoshop CS5	Adobe Systems, USA
Autodesk Maya 2011	Autodesk Inc., USA
LaTeX	`http://www.latex-project.org/`
Image J 1.43	Wayne Rasband (NIH) `http://rsbweb.nih.gov/ij/index.html`
SPSS for Windows 11.5.1	SPSS/ IBM, NY, USA
Microsoft Office 2003	Microsoft Deutschland, Berlin, Germany

Table 2.7 – Computer Software

2.2. Methods

2.2.1 Transgenic animals

cd39$^{-/-}$ mice on the C57BL/6x129svj background were kindly donated by Simon Robson (Enjyoji et al., 1999), from the Department of Gastroenterology of the Harvard Medical School (Boston, MA, USA). As controls, wild type C57BL/6x129svj mice were selected. *cd73* $^{-/-}$ mice were described previously (Castrop et al., 2004) and were kindly provided by Dr. Jurgen Schnermann, NIDDK, Bethesda. Wild type C57BL/6 were used as controls for experiments with these mice. All animals were bred in the animal facility of our institute. The experiments were conducted in accordance with the German guidelines for animal care and approved by the local legal authorities (Tötungsgenehmigung T0014/08).

2.2.2 Genotyping of CX3CR1$^{+/-}$-eGFP mice

A piece of 2-10 mm length was cut from the tail tip of at least 4 weeks old mice and placed in 100 µl Direct PCR-Tail lysis buffer with 10 µl of Proteinase K (PeqLab, Erlangen, Germany). Tissue was left at 55°C on a shaker for 3h. The lysis was stopped 45 min of incubation at 85°C. After the centrifugation at 16000 g for 10 min, the supernatant was kept at -20°C until used for PCR. PCR reagents were mixed as following:

ddH_2O	17.25 µl
$MgCl_2$	1.5 µl
Primer forward *IMR 3946* (25 µM)	0.5 µl
Primer reverse *IMR 3947* (25 µM)	0.5 µl
dNTP (10 mM)	0.5 µl
10 x reaction buffer	2.5 µl
Tail DNA	2.0 µl
Taq polymerase Invitrogen	0.25 µl

Table 2.8 – PCR Mix for eGFP knockin mice

ddH_2O	17.25 µl
$MgCl_2$	1.5 µl
Primer forward *IMR 3946* (25µM)	0.5 µl
Primer reverse *IMR 3946* (25 µM)	0.5 µl
dNTP (10 mM)	0.5 µl
10 x reaction buffer	2.5 µl
Tail DNA	2.0 µl
Taq polymerase Invitrogen	0.25 µl

Table 2.9 – PCR Mix for CX3CR1$^{+/-}$

Reaction	**Temperature, °C**	**Time**
Initial Denaturation	94	3 min
35 Cycles:		
Denaturation	94	30 sec
Annealing/ Elongation	60	30 sec
Polymerisation	72	2 min
Final polymerisation	72	2 min

Table 2.10 – PCR program for genotyping CX3CR1$^{+/-}$-eGFP mice

The products of the PCR were then loaded on the 1.5 % agarose gel with 0.5 µg/ml ethidium bromide and were subjected to the electrophoresis in TAE running buffer. The separated fragments were analyzed under the UV light (254 nm).

2.2.3 Genotyping of CD39$^{+/+}$ and CD39$^{-/-}$ mice

Genotyping of the *cd39*$^{-/-}$ mice was performed according to the following protocol. A piece of 2-10 mm length was cut from the tail tip of at least 4 weeks old mice and placed in 100 µl Direct PCR-Tail lysis buffer with 10 µl of Proteinase K (PeqLab, Erlangen, Germany). Tissue was left at 55°C on a shaker for 3h. The lysis was stopped 45 min of incubation at 85°C. After the

centrifugation at 16000 g for 10 min, the supernatant was kept at -20°C until used for PCR. PCR reagents were mixed as following:

ddH_2O	15.75 µl
Primer forward *D3M* (25 µM)	0.5 µl
Primer reverse *MEC8P* (25 µM)	0.5 µl
dNTP (10 mM)	0.5 µl
10 x reaction buffer	2.5 µl
Tail DNA	5.0 µl
TaKaRa Ex Taq polymerase	0.25 µl

Table 2.11 – PCR Mix for $CD39^{+/+}$ mice

ddH_2O	15.75 µl
Primer forward *D3M* (25 µM)	0.5 µl
Primer reverse *NEOP2* (25 µM)	0.5 µl
dNTP (10 mM)	0.5 µl
10 x reaction buffer	2.5 µl
Tail DNA	5.0 µl
TaKaRa Ex Taq polymerase	0.25 µl

Table 2.12 – PCR Mix for $CD39^{-/-}$ mice

Reaction	**Temperature, °C**	**Time**
Initial Denaturation	94	1 min
30-33 Cycles:		
Denaturation	94	15 sec
Annealing/ Elongation	66	30 sec
Polymerisation	72	3 min
Final polymerisation	72	2 min

Table 2.13 – PCR program for genotyping $CD39^{+/+}$ and $CD39^{-/-}$ mice

The products of the PCR were then loaded on the 1.5 % agarose gel with 0.5 µg/ml ethidium bromide and were subjected to the electrophoresis in TAE running buffer. The separated fragments were analyzed under the UV light (254 nm).

2.2.4 Genotyping of CD73$^{+/+}$ and CD73$^{-/-}$ mice

Cd73 $^{-/-}$ mice were described previously (Castrop et al., 2004). Briefly, the genotyping protocol was the following. A piece of 2-10 mm length was cut from the tail tip of a, at least, 4 weeks old mice and placed in 100 µl Direct PCR-Tail lysis buffer with 10 µl of Proteinase K (PeqLab, Erlangen, Germany). Tissue was left at 55°C on a shaker for 3h. The lysis was stopped 45 min of incubation at 85°C. After the centrifugation at 16000 g for 10 min, the supernatant was kept at -20°C until used for PCR. PCR reagents were mixed as following:

ddH_2O	17.75 µl
DMSO	1.0 µl
Primer forward *SC3* (25 µM)	0.5 µl
Primer reverse *SC4* (25 µM)	0.5 µl
dNTP (10 mM)	0.5 µl
10 x reaction buffer	2.5 µl
Tail DNA	2.0 µl
Roché Taq polymerase	0.25 µl

Table 2.14 – PCR Mix for CD73$^{+/+}$ mice

ddH_2O	17.75 µl
DMSO	1.0 µl
Primer forward *NeoRS* (25 µM)	0.5 µl
Primer reverse *NeoRas* (25 µM)	0.5 µl
dNTP (10 mM)	0.5 µl
10 x reaction buffer	2.5 µl
Tail DNA	2.0 µl
Roché Taq polymerase	0.25 µl

Table 2.15 – PCR Mix for $CD73^{-/-}$ mice

Reaction	**Temperature, °C**	**Time**
Initial Denaturation	94	5 min
34 Cycles:		
Denaturation	94	45 sec
Annealing/ Elongation	58	45 sec
Polymerisation	72	45 sec
Final polymerisation	72	8 min

Table 2.16 – PCR program for genotyping $CD39^{+/+}$ and $CD39^{-/-}$ mice

The products of the PCR were then loaded on the 1.5 % agarose gel with 0.5 µg/ml ethidium bromide and were subjected to the electrophoresis in TAE running buffer. The separated fragments were analyzed under the UV light (254 nm).

2.2.5 Astrocytes-microglia co-culture and microglia isolation

Microglial cultures were prepared from whole brains of P0-P1 mice as described previously (Prinz et al., 1999). The full brains of 0 to 1-day old pups were removed and carefully freed of blood vessels and meninges. Brains were then washed 3 times with HBSS and treated (except for olfactory bulb and cerebellum) with trypsin (10 mg/ ml PBS) and DNase (0.5 mg / ml PBS)

for 2 min. The reaction was stopped by the addition of 10 ml Dulbecco's modified Eagle's medium (DMEM), supplemented with 10% fetal calf serum (FCS). After the removing the excess of medium, tissue was dissociated with a fire-polished pipette and DMEM was added to 15 ml of total volume. Cells were then washed by centrifugation for 10 min, 1000 g at 4°C. Mixed glial cells were cultured for 9 to 12 days in DMEM, supplemented with 10% fetal calf serum (FCS), 2 mM L-glutamine and antibiotics (100 U/ml penicillin and 100 µg/ml streptomycin, PSG), with medium changes every third day. For further preparation of pure microglial cells, medium was changed to supplemented DMEM with $^1/_3$ volume of conditioning medium of L929 fibroblasts. After 2-3 days first microglia was separated from the underlying astrocytic monolayer by gentle shaking of the flasks for 1 h at 37°C in a shaker-incubator (100 rpm). Addition of L929 conditioning medium ensured 3 consequent dissociations of microglia from the astrocytic layer with the 2-3 days intervals. The cells were seeded in 24-well plates or 96-well plates at a density of 2×10^5 or 1×10^4 cells per well, respectively. Cultures usually contained >95% microglial cells, identified by positive staining with Griffonia simplicifolia isolectin B_4 (Sigma, Deisenhofen, Germany), a marker for microglia. Cultures were used for experiments 1 to 2 days after plating.

2.2.6 Primary astrocytic culture

Upon shaking off primary microglia, astrocytic monolayer was trypsinized and seeded into the 96-well plate at the density of 1-2×10^4 per well. The medium for astrocytes cultivation was DMEM medium supplemented with FCS and antibiotics as described above. Astrocytes were then kept in incubator for at least 24 h until further measurement of extracellular ATP degradation by means of Malachite Green phosphate assay (see section 3.3.1). For one of the experiments, astrocytes were pre-treated with clodronate (Markovic et al., 2005) to ensure complete microglia removal.

2.2.7 Preparation of acute brain slices

Preparation of acute brain slices was performed as previously described (Brockhaus et al., 1993). Depending on the experimental design, either young P6-P9 or adult mice (6-18 weeks) were used. After decapitation, forebrain

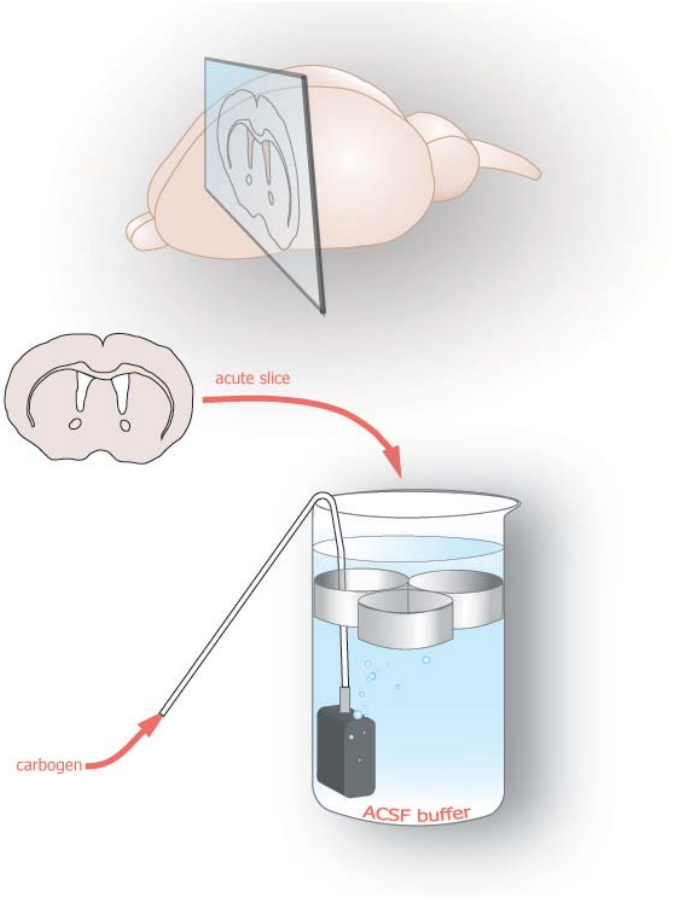

Figure 2.1 – Preparation of acute brain slices.
Coronal brain slices were carefully transferred onto the nylon grid in the ACSF (room temperature) continuously saturated with carbogen (95% CO_2, 5% O_2). Acute brain slices can be kept in ACSF, saturated with carbogen, for up to 6h without significant damage to microglia. © *L. Bulavina.*

hemispheres were quickly isolated and shortly washed in the ice-cold ACSF buffer. Immediately after, brains were mounted and cut into the coronal slices with vibratome (HM650V, MICROM GmbH, Walldorf, Germany). 250 µM-thick cortical slices were cut in ice-cold artificial cerebrospinal fluid solution (ACSF) buffer (Schipke et al., 2008). Slices were then carefully transferred onto the nylon grid in the ACSF (room temperature), continuously saturated with carbogen (95% CO_2, 5% O_2) (Fig. 2.1). In our experience, acute brain slices can be kept in ACSF, saturated with carbogen, for up to 6 h without significant damage to microglia. For practical reasons, 2 h of slices preservation in ACSF was used as a standard in my experimental approach.

2.2.8 Measurement of extracellular ATP degradation in astrocytic and microglial primary cultures using Malachite Green phosphate assay

Free orthophosphate, $[PO_4^{3-}]$, is released to the extracellular medium by microglial and astrocytic cells at basal levels and it is mostly due to the enzymatic cleavage of the extracellular purines. Using a Malachite Green phosphate assay (BioAssay Systems), we were able to estimate the free orthophosphate concentration in the reaction buffer under the experimental conditions. Briefly, this assay is based on quantification of the green complex between malachite green, molybdate and free orthophosphate. The color of the formation is, therefore, proportional to the phosphate concentration and it can be colorimetrically measured on a spectrophotometer (Tecan i-control, infinite). Thus, we evaluated the activity of CD39 and CD73 on microglia and astrocytes by adding 1mM ATP, 1mM ADP or 1mM AMP solutions (100 µl per well, 96 well format) to the cultures (5×10^4 cells/well or 250 µm-thick brain slice per well). In parallel, the solutions of ATP, ADP, AMP and reaction buffer were added into the new 96 well plate without any cells for controlling the spontaneous degradation of purines or any free phosphate contaminations in the solutions. After 10 minutes of incubation at 37°C, reaction was stopped by adding 20 µl of 10% TCA to 90 µl of either cell supernatant or control solutions and placed on ice. Next, the samples were diluted 1:5 with phosphate-free reaction buffer, pH 7.4 to prevent precipitation or signal saturation. Phosphate standards were prepared for the calibration. 80 µl of test samples and standards were transferred into the separate wells of 96 well plate. The working reagent was prepared according to the protocol instructions by mixing the Reagent A and Reagent B at the 1:100 ratio. 20 µl of working reagent per well was finally added to the samples and standards and the chromogenic reaction was developed within 30 minutes at room temperature. The final optical density (OD) was measured on Tecan spectrophotometer at 620 nm. OD620nm was then plotted versus standard phosphate concentrations. Sample phosphate concentrations in µM were determined from standard curve. For the final expression of enzymatic activity, free phosphate concentrations were normalized to the corresponding amount of protein. Enzymatic activity was then calculation

according to the definition as:

$$A = \frac{[PO_4^{3-}]}{M \times t} \tag{2.1}$$

where A is the enzimatic activity in $\mu mol \cdot mg^{-1} \cdot min^{-1}$, $[PO_4^{3-}]$ is the phosphate concentration measured in the buffer in µmol, M in the protein mass in mg and t is the time in $minutes$.

2.2.9 Protein measurement in microglial and astrocytic primary cultures using BCA Kit

The BCA assay (Thermo Scientific) is biochemical assay used for determining the concentration of a protein in a solution. It is mainly based on the reaction of bicinchoninic acid (BCA) with the reduced (cuprous, Cu^+) cation. On the first reaction, the peptide bounds of the protein reduce the Cu^{2+} ions from the $CuSO_4$ (cupric sulfate) present in the solution to form Cu^+ ions in an alkaline environment (biuret reaction). The amount of Cu^{2+} reduced is therefore proportional to the amount of protein present in the solution. In the second reaction, two molecules of BCA chelate with one Cu^+ ion, forming an intense purple-colored reaction product that absorbs light at a wavelength of 562 nm. To isolate the protein from microglia and astrocytes, cells were lysed with 0.02% w/v SDS (50 µl per well in 96-well plates) for 20 minutes at room temperature and agitation. Estimation of the protein concentration was performed afterwards according to the kit instructions. Consequently, 25 µl of each standard and unknown sample were placed into the separate wells of microplate and 200 f the working reagent (a mix of 50 parts of Reagent A with 1 part of Reagent B) was added per well. The reaction was developed over 30 min in a wet chamber at 37°C. The plate was cooled to room temperature and the absorbance was measured at 562 nm on Tecan spectrophotometer. The optical density (OD562 nm) of each sample was then plotted against standard BSA concentrations and sample protein concentrations in mg/ml were determined from the standard curve.

2.2.10 Preparation and handling of organotypic brain slices

The procedure to establish organotypic brain slice cultures is a modification of previously published protocols (Schipke et al., 2008). Brain tissue was derived from 16th to 21st day-old C57BL/6 mice (animal breeding facility, Schönewald, Germany). For organotypic brain slice preparations, mice were decapitated according to the regulations from the Landesamtes für Gesundheit und Soziales Berlin (LAGeSo). Brain was quickly removed and placed in ice-cold (4°C) phosphate-buffered saline (PBS) under sterile conditions. The forebrain was dissected from the brainstem and glued (using cyanoacrylate glue) onto a metal pad and cut in the coronal plane into 250 µm sections with a vibratome (Leica VT1000S; Leica Co., Heidelberg, Germany). The brain slices were transferred onto the 0.4 µm polycarbonate membrane in the upper chamber of a transwell tissue insert (Falcon model 3090; Becton Dickinson), which was inserted into a 6-well plate (Falcon model 3502; Becton Dickinson) with 1 mL of culture medium per well (Fig. 2.2). The brain slices were kept in sterile conditions at 37°C, 5% CO_2 and 100% humidity. After overnight equilibration of the brain slices in culture medium, the slices were exchanged for cultivation medium (see table 2.2), which was carefully added directly into the wells and not in the inserts. Cultivation medium was then changed each second day.

2.2.11 Depletion of microglia in organotypic brain slices

Microglia depletion was performed as previously described (Markovic et al., 2005). Briefly, clodronate-filled liposomes were diluted 1:10 with culture medium. The medium in the wells of the organotypic slices was exchanged to the clodronate-liposomes-containing culture medium (1 ml per well in a 6-well plate). Organotypic brain slices were then incubated in clodronate-liposomes-containing culture medium for minimum 24 h for efficient ablation of the microglia. After this time, clodronate-containing medium was removed and substituted with cultivation medium. Organotypic brain slices were left in cultivation medium for the next 72 h to circumvent any false effects due to reactive astrocytes.

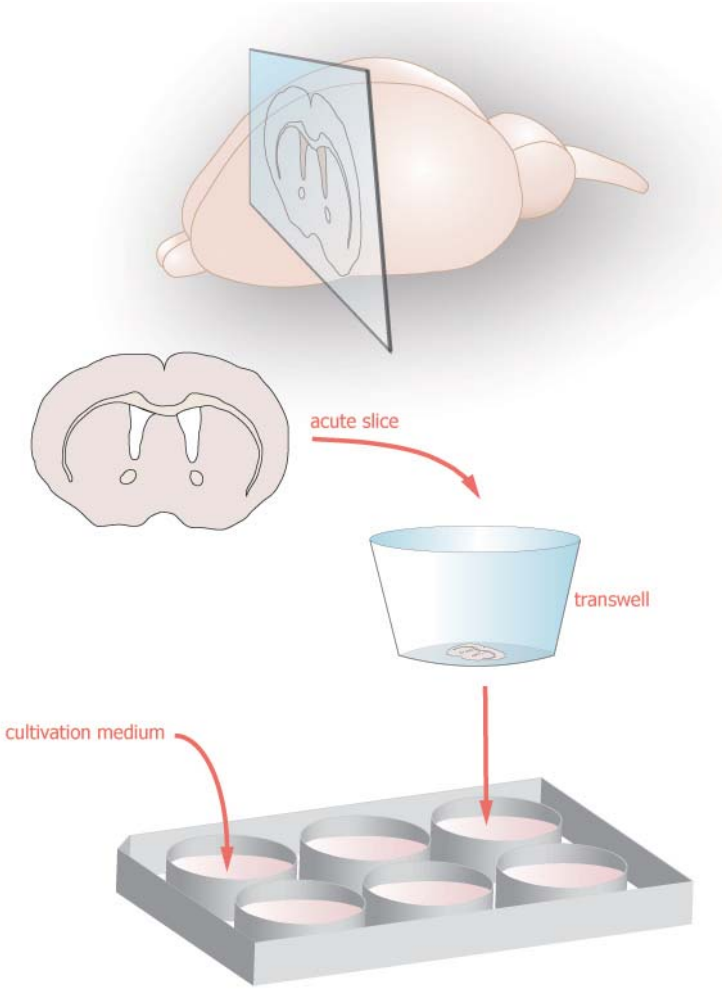

Figure 2.2 – Preparation of organotypic brain slices.
250 µM thick coronal brain slices were carefully placed in the middle of the transwell and in the 1 ml of culture medium in a 6-well plate. Cultivation medium was changed each second day. © *L. Bulavina.*

2.2.12 Measurement of extracellular ATP degradation in the organotypic slices using Malachite Green phosphate assay

For each experiment we compared clodronate-treated slices against non-treated control slices with preserved microglia. Because organotypic slices are extremely fragile and tend to brake into pieces when removed from their polycarbonate substrate, slices were carefully cut out together with the membrane and placed into the 0.5 ml of reaction buffer in a 24-well plate. Thus, the volume of reaction buffer was 5 times increased, which was considered later

in the data analysis. The rest of the procedure was carried out as described above (see 3.3.1). For the final expression of enzymatic activity, free phosphate concentrations were normalized to the corresponding amount of protein (see 2.2.9). Enzymatic activity was then presented as in equation 2.1.

2.2.13 *In situ* phagocytosis assay with pHrodo labeled *E. coli* bioparticles

Acute brain slices of CX3CR1-eGFP mice (6-20 weeks old) were prepared as described above (see section 2.2.7). Immediately after the preparation, HBSS working solution with *E. coli* bioparticles was prepared. Briefly, a single ready-to-use tube of lypophilized particles from provider (Invitrogen) was diluted in 6 ml of HBSS, vortexed and sonicated. 3 ml of bioparticles solution were then spinned down and resuspended in 1 ml of FCS for opsonization (30 min at room temperature). After the incubation with FCS, *E. coli* bioparticles were spinned down and resuspended again in 3 ml of HBSS. Brain slices were then placed in 24-well plates. Because the intensity of the pHrodo signal increases only upon internalization and phagosome acidification, while kept unchanged in buffered solution, no washing steps prior to the measurement are required. The bioparticles internalisation was assessed using two-photon microscopy.

2.2.14 *In situ* phagocytosis assay with opsonized latex microspheres

Preparation of acute brain slices was performed as described above (See section 2.2.7). After the slice preparation, 10 µl of green-fluorescent latex beads (Polysciences Inc, Fluoresbrite® Yellow Green (YG) Carboxylate Microspheres, 1.68×10^9 particles/ml) were opsonized by incubating with 1 ml of FCS (Gibco) at room temperature and agitation for 30 minutes. Opsonized beads were spinned down and resuspended in 1 ml of HBS. For phagocytosis measurement, 2 h pre-incubated acute slices were transferred into the 24-well plate (1 slice per well). 0.5 ml HBS solution with beads was added per well and slices were incubated for the next 1 h at 37°C with slight agitation (Fig. 2.3). Finally, slices were washed 3 times with ice-cold PBS, fixed with 4% PFA (1h at room temperature) and immunostained for Iba1 microglia marker. To evaluate the

phagocytic activity of microglia in acute brain slices, cortex was chosen as the main region of interest and submeningeal, periventricular and perivascular areas were excluded from analysis.

2.2.15 Image acquisition and analysis of the phagocytosis assay

Confocal laser scanning microscopy was performed on Leica TCS SP5 with 40x oil immersion objective (Leica, Wtzlar, Germany). We acquired 20 µm-thick z-stacks at 0.5 µm interval beginning from the slice surface in the cortex area of each slice. Total amount of engulfed beads per cells, number of phagocytic microglia and total number of microglia cells were counted in each z-stack using Image J software. Only beads colocalized in individual optical section with Iba1-positive microglia cells were counted as phagocytosed. The phagocytic index was calculated for each confocal stack by multiplying the percentage of phagocytic cells with average number of beads per phagocytic cell. Results were presented as *"number of phagocytosed beads per 100 cells"* or shortly as *beads/100×cell*.

2.2.16 Pharmacological block of P1 and P2 receptors

For experiments with pharmacological compounds, either 100 µM PPADS (pyridoxal-5'-phosphate-6-azophenyl-2,4-disulfonate) or 10 µM NECA (1-(6-amino-9H-purin-9-yl)-1-deoxy-*N*-ethyl-β-D-ribofuran-uronamide) were diluted in microspheres suspensions before addition to the slices.

2.2.17 Iba1 immunostaining of microglia in acute brain slices

4% PFA fixed (1 h at room temperature) and washed brain slices were incubated 4 h in permeabilisation buffer (2% Triton X-100, 2% BSA, 10% NGS in 0.1M PB, pH 7.4), followed by 48 h of incubation with 0.75 $\mu g/ml$ Iba1 (Waco) in dilution buffer (1:10 of permeabilisation buffer in 0.1 M PB pH 7.4) at 4°C, followed by incubation with goat anti-rabbit Alexa 633 (Molecular Probes, Invitrogen) (4 µg/ml in dilution buffer) for 2h at room temperature. After washing, slices were mounted in Aqua-Poly/Mount (Polysciences Inc) and kept 24 at room temperature for polymerization of mounting medium.

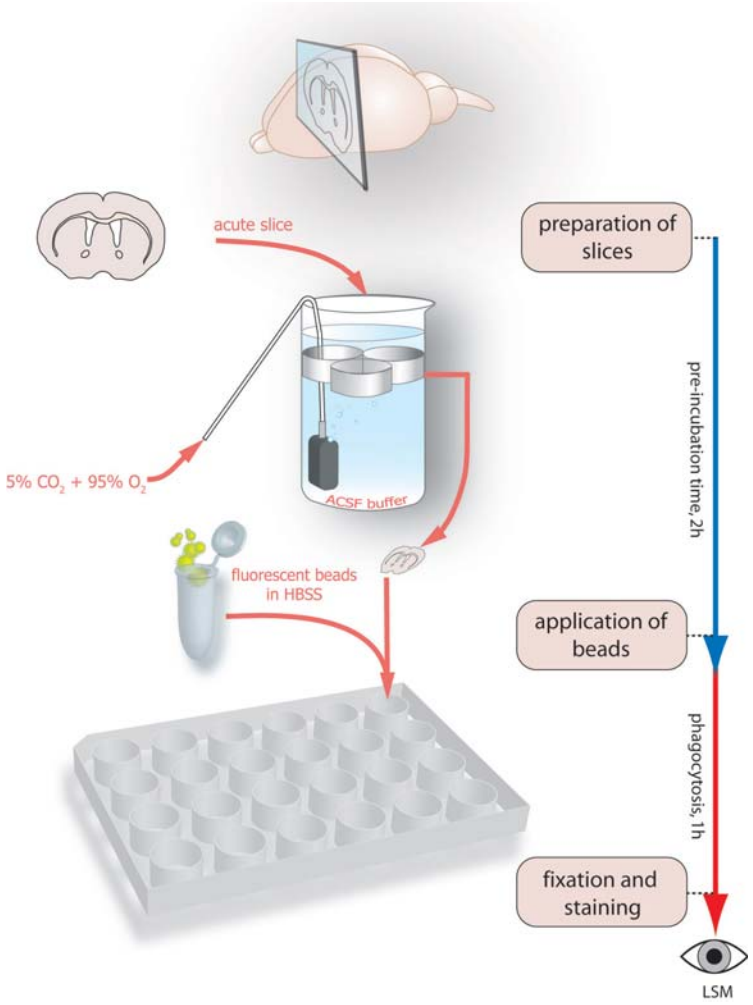

Figure 2.3 – ***In situ*** **phagocytosis assay with opsonized latex microspheres.** Forebrain hemispheres of freshly isolated brain of 6-18 weeks old mice were cut into 140 µm thin coronal slices with a vibratome in ice-cold ACSF buffer. Slices were transferred onto a nylon grid incubated in ACSF, continuously supplied with carbogen (95 % CO_2, 5 % O_2) for 2h. 500 µl of a suspension containing 8.4×10^6 yellow-green fluorescent carboxylated microspheres were applied on each acute brain slice and incubated for 60 min at 37 °C. Afterwards, brain slices were fixed and immunostainned with Iba1 antibody and examined with a confocal laser scanning microscope. © *L. Bulavina.*

2.2.18 Transient endovascular filament middle cerebral artery occlusion

The technique of endovascular filament (intraluminal suture) middle cerebral artery occlusion (MCAO) as an animal model of ischemic stroke was described first by Koizumi (Koizumi et al., 1986) and modified by Endres and Laufs (Endres et al., 1998). The experimental work was performed in col-

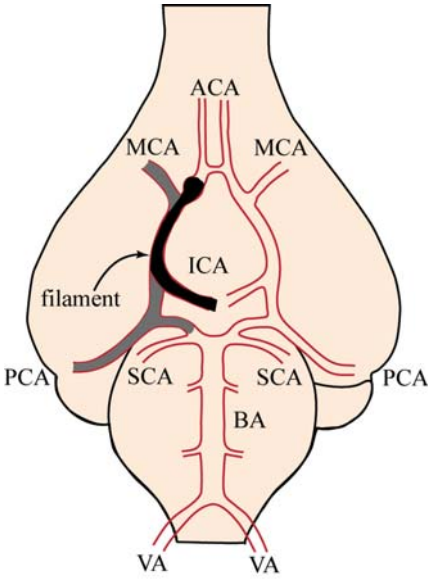

Figure 2.4 – Filamentous middle cerebral artery occlusion (MCAO) in B6 mouse.
Ischemic stroke was provoked by temporal occlusion of the internal carotid artery with a filament for 60 min. MCA - medial cerebral artery; ACA - anterior cerebral artery; ICA - internal carotid artery; PCA - posterior cerebral artery; VA - vertebral artery; BA - basilar artery; SCA - subcerebellar artery.

laboration with Dr. Vincent Prinz (Department of Experimental Neurology, Charité). Shortly, 6 weeks old B6 mice were anesthetized by 1.0% (vol/vol) isoflurane in 69% nitrous oxide (N_2O) and 30% oxygen (O_2) administered via a facemask. Focal cerebral ischemia was induced with an 8.0 nylon monofilament coated with a silicone resin/hardener mixture (Xantopren M Mucosa and Activator NF Optosil Xantopren, Haereus Kulzer, Germany) by introduction of the filament into the left internal carotid artery up to the anterior cerebral artery. Thereby, the middle cerebral artery and anterior choroidal arteries were occluded (Fig. 2.4). Filaments were withdrawn after 60 min to allow reperfusion. Rectal temperature was controlled and kept constant at 36.5±0.5°C. Regional cerebral blood flow (rCBF) was measured by means of a flexible probe and laser-Doppler monitoring (Perimed). There was an equivalent drop in rCBF to less than 20% of baseline at filament insertion and an equivalent rise in rCBF at filament withdrawal. 48 h after the MCAO onset, mice were decapitated and acute slices were prepared for further phagocytosis assay with opsonized latex microspheres.

2.3. Statistical Analysis

One-way ANOVA test, followed by post hoc paired t-tests with Bonferroni correction or t-test were used for statistical analysis. Values are presented as mean ± SEM. In every figure, error bars corresponds to the S.E.M. Stars are

used to represent the significant value from the test according to the following scheme (Table 2.17):

Symbol	**p-value**
*	p<0.05
**	p<0.01
***	p<0.001

Table 2.17 – Statistical Significance

CHAPTER 3

Results

3.1. Microglia is a major provider of P2 and P1 substrates in the CNS

CD39, mainly expressed by microglia, is the major ectoenzyme, degrading extracellular ATP and ADP in the CNS. However, other ectoenzymes expressed in the CNS (such as TNAP and NPP, see 1.2.5 and 1.2.5) can as well participate in ATP degradation. The role of CD73 in AMP hydrolysis is expected to be more exclusive. In the following set of experiments I evaluated the redundancy of CD39 and CD73 functions, using corresponding knockout animals. Both primary glial cells and acute brain slices were used to measure the hydrolysis of externally applied ATP, ADP or AMP. Primary microglia and astrocytes were isolated from C57/BL6 new-born mice as described in 2.2.5 and 2.2.6. Acute brain slices of adult wild type, *cd39*$^{-/-}$ and *cd73* $^{-/-}$ mice were prepared on the day of experiment as described in 2.2.7. To determine the concentration of free orthophosphate, resulted from the cleavage of externally applied ATP, ADP or AMP solutions, we used Malachite green phosphate assay (3.3.1 and 2.2.12).

3.2. Microglial cells have higher extracellular ATP-degrading activity than astrocytes

According to the present knowledge, ATP signaling in the brain needs to be tight controlled for a content inflammatory response. However, how the homeostasis of ATP is performed in the brain and what the relevance for microglial function would be is still unclear. In these experiments we aimed thus at studying the relevance of microglia function regarding ATP homeostasis in the CNS.

ATP homeostasis is thought to be done mainly by the action of the ectonucleotidases. These are expressed in all main cellular types of the CNS, such as neurons, astrocytes, microglia and blood vessels. However, each of them expresses different types of endonucleotidases. Therefore, each of the cells may participate differently in ATP homeostasis in the brain. From all the cells, astrocytes and microglia seems to be of greater importance for that, since they express the endonucleotidases with fastest kinetics for ATP removal. Astrocytes mainly expresses E-NTPDase2, which dephosphorilases ATP to ADP leading to ADP accumulation. Microglia expresses, on the other hand, E-NTPDase1, which is not restricted to ATP phosphorilation but also cleaves ADP causing a fast degradation of all possible activators of P2X and P2Y. Therefore, we first compared which of both cellular types might be the most likely candidate to have a more important role in ATP homeostasis in the brain.

For that, we assessed the activity of extracellular enzymes degrading purine-phosphates in purified cell cultures of mouse brain astrocytes or microglia. Cell cultures were incubated with 1 mM ATP or ADP for 10 min and free phosphate released from the dephosphorylation of these substrates was measured in the supernatant using Malachite Green assay (Geladopoulos et al., 1991 and section 3.3.1). Protein content was used in all the measurements as reference. Two control conditions were considered for the assay. In the first one, direct release of phosphate by culture cells was evaluated by measuring the basal phosphate concentration in cultures depleted from ATP and ADP. Secondly, the contribution of non-enzymatic degradation of ATP and ADP was estimated by incubating culture medium with ATP and ADP in absence of

cells. The levels of phosphate measured in these controls were accordingly subtracted from the experimental values.

The results showed that both astrocyte and microglia cultures were able to generate free phosphate from ATP and ADP. However, phosphate production differed enormously depending on the cell type. Phosphate production from ATP was nearly 3 times higher in cultures of microglia than of astrocytes, namely 8.07 ± 0.37 (n=46) and 2.96 ± 0.18 μmol phosphate/mg protein/min (n=34) (***) correspondingly. Higher differences were observed when we measured the phosphate levels obtained from ADP. Here, microglia cultures exhibited an enzymatic activity of 5.11 ± 0.43 (n=38) whereas astrocytes activity was only 0.74 ± 0.07 μmol phosphate/mg protein/min (n=26) (***) (Fig. 3.1a). To exclude a contamination by microglia in astrocytic cultures (Saura, 2007), we also measured phosphate release by astrocyte cultures pretreated for 72 h with clodronate, which selectively kills microglia (Markovic et al., 2005). Here the enzymatic release of phosphate from ATP and ADP was similar in clodronate-treated as compared to untreated cultures. The enzymatic activity for ATP was 2.66 ± 0.08 (n=11) and 2.96 ± 0.18 μmol phosphate/mg protein/min (n=34) (***) correspondly and the one for ADP was 1.25 ± 0.36 (n=11) and 0.74 ± 0.07 μmol phosphate/mg protein/min (n=26) (***), respectively (Fig. 3.1a). Although microglia seemed to dephosporilate AMP as well faster than astrocytes, no significant difference was detected in AMP degradation between both cell types.

In summary, the astrocytic efficacy of purines degradation was significantly reduced to 36.63 ± 2.18 % , 14.56 ± 1.31 % , and 10.68 ± 4.08 % of microglial ATP, ADP and AMP degradation efficacy (100%) correspondingly (***) (Fig. 3.1b).

3.3. Impact of CD39 expression on ATP and ADP dephosphorylation in microglia cultures and brain tissue

From the previous results, we see that, in fact, microglia is the cell type with fastest kinetics for ATP removal of the brain. Microglia dephosphorylation activity is very likely to be dependent on E-NTPDase1 (CD39), since this endonucleotidase has the lowest K_m for ATP dephosphorylation. Therefore, we examined if ATP homeostasis was impaired in CD39-depleted brain slices.

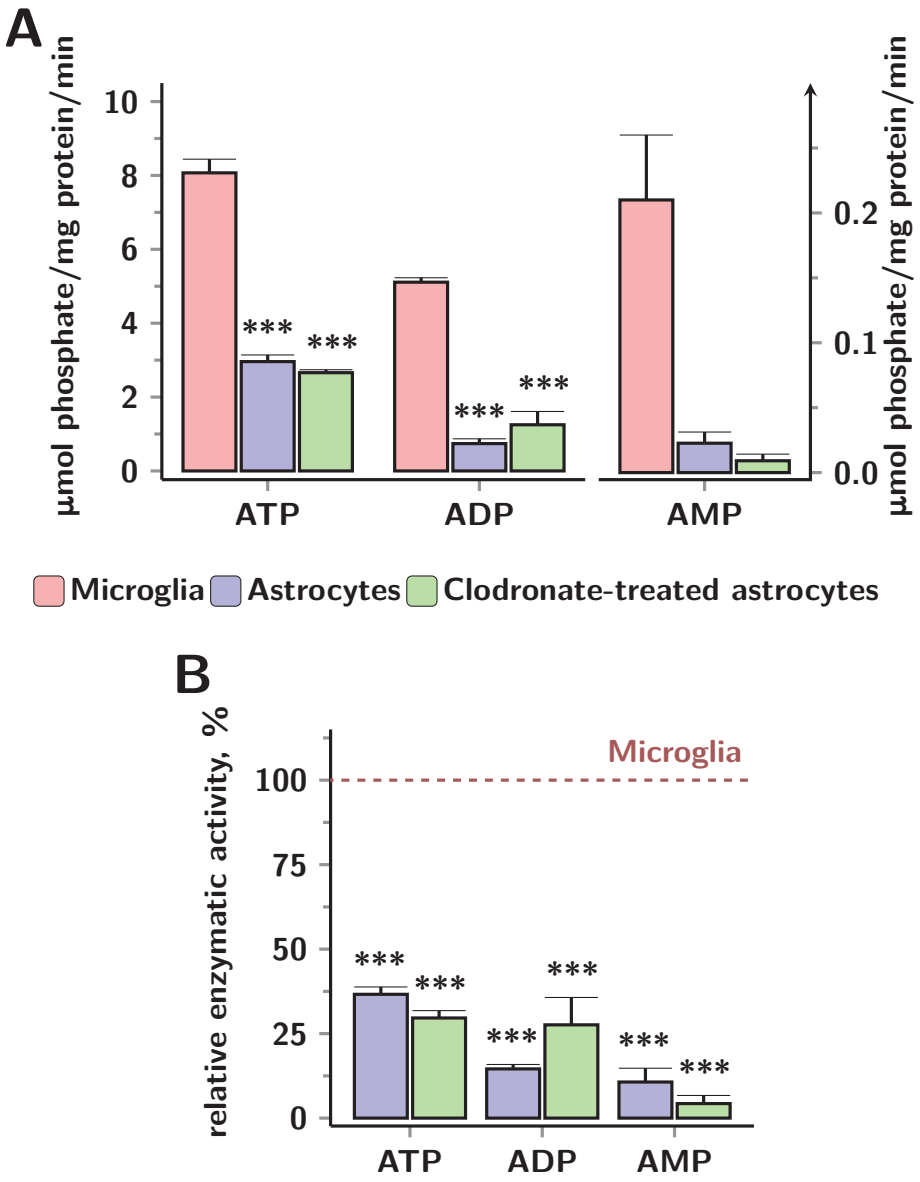

Figure 3.1 – Microglia dephosphorilate extracellular ATP and ADP more efficiently than astrocytes.
A. Specific enzymatic activities of extracellular ATP- and ADP-degrading enzymes are higher in primary cultures of microglia ( ) compared to astrocytes ( ). Enzymatic activity in astrocytes could not be caused by microglial contamination, since microglial removal after clodronate treatment did not change dephosphorilation efficiency ( ). **B.** Same data as above normalized to microglial enzymatic activity .

3.3.1 CD39 is responsible for the extracellular dephosphorylation of ATP and ADP *in vitro*

It is known that dephosphorylation of triphophonucleotides and diphosphonucleotides in microglia is mainly dependent on the ectonucleotidases fam-

ily (see section 1.2.2). From all, the E-NTPDase1, also called CD39, presents a very high kinetic activity for both species (see section 1.2.3) and it is, therefore, believed to be the main player in the removal of ATP and ADP. Consequently, we followed next to examine how CD39 may affect the extracellular dephosphorylation of ATP and ADP. For this purpose, we measured the dephosphorylation activity as performed in the previous experimental procedure (see section) in a *cd39*$^{-/-}$ background.

Interestingly, in microglia cultures from *cd39*$^{-/-}$ animals, generation of phosphate from ATP was almost absent in comparison with cultures obtained from control animals (0.12 ± 0.07 and 3.12 ± 0.53 µmol phosphate/mg protein/min (***), respectively). Similarly, dephosphorylation of ADP was profoundly impaired in absence of CD39 as compared to the wild type phenotype (0.14 ± 0.05 (n=15) and 1.95 ± 0.49 µmol phosphate/mg protein/min (***), respectively; Fig. 3.2a). The efficacy of ATP and ADP degradation by CD39-deficient microglia was indeed reduced to 3.88 ± 2.26 % and 6.58 ± 2.72 % as compared to control microglia (***) (Fig. 3.2b).

This indicates that CD39 is the major enzymatic component of microglia for the degradation of ATP and ADP.

3.3.2 Extracellular ADP removal in the brain is mainly done by a CD39-dependent dephosphorylation

Based on the previous experiment, we believe that ATP removal is produced by microglia by a CD39-dependent dephosphorylation. However, it is known that the microglial population in the brain is very small when compared to the one of astrocytes. It could mean that even with reduced dephosphorylation capabilities, the overall astrocytic population of the brain could take responsibility of the ATP removal in absence of microglia. Furthermore, other known cell types with minor dephosphorylation abilities, such as neurons and blood vessels, could be also important in ATP homeostasis due its high number in the brain. Therefore, we next aimed at examining ATP buffering in the brain tissue.

In the following experiment, we tested the importance of CD39-mediated dephosphorylation of triphophonucleotides and diphosphonucleotides in brain tissue. Similarly to the experiments *in vitro*, dephosphorylation of ATP and

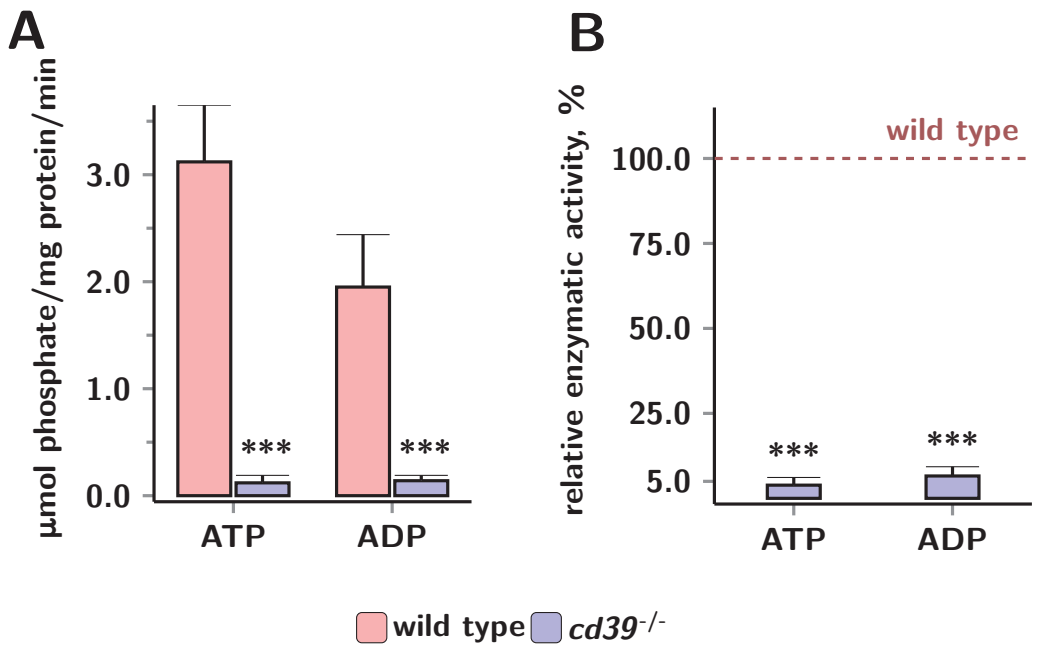

Figure 3.2 – Dephosphorilation of ATP and ADP in absence of CD39 is only residual in microglial cultures.
A. CD39 deficient microglial cells ( ) were virtually incapable of ATP and ADP degradation in culture as compared to control animals ( ). Specific enzymatic activity of extracellular ATP- and ADP-degrading enzymes was nearly null when compared to astrocytes. **B.** Same data as above normalized to control enzymatic activity .

ADP was reduced in absence of *cd39*. However, this reduction was statistically significant only for ADP degradation in *cd39*$^{-/-}$ animals in comparison with wild types. In fact, whereas ADP derived phosphate production decreased from 5.80 ± 0.73 in control acute brain slices to in 2.69 ± 0.59 µmol phosphate/mg protein/min in *cd39*-depleted preparations (***), ATP dephosphorylation changed only from 9.29 ± 0.88 (n=15) to 7.07 ± 0.65 µmol phosphate/mg protein/min (n=15), respectively (Fig. 3.3a).

The fact that ATP can still be successfully degraded by brain tissue in the absence of CD39 can be explained by the activity of other dephosphorilases such as TNAP and NPPs, which are expressed by astrocytes, brain vasculature and neurons (see section 1.2.5). However, our results indicate that the function of CD39 in diphosphonucleotides dephosphorylation cannot be fully compensated by other brain mechanisms. According to these results, microglia, by a CD39-dependent mechanisms, is most likely to be the only responsible of the buffering of ADP. The resultant accumulation of AMP may have very important consequences in the regulation of the brain inflammatory response.

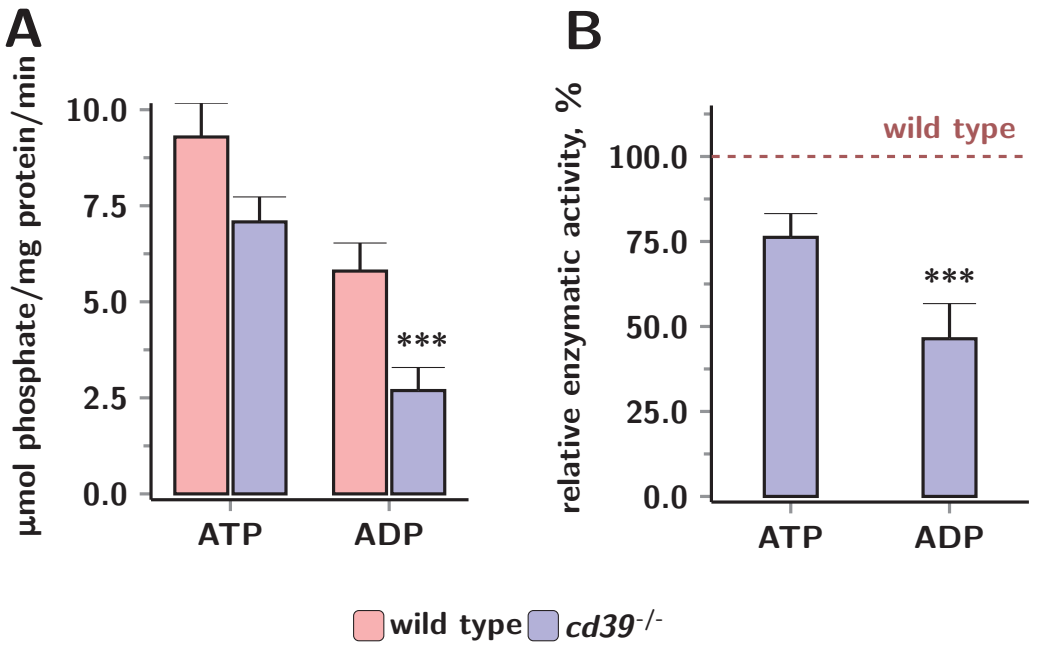

Figure 3.3 – Impaired microglial nucleoside dephosphorilation is partially compensated in brain tissue.
A. Enzymatic activity for ATP and ADP dephosphorilation in brain slices. Alternative brain mechanisms can produce ATP degradation in absence of CD39-dependent microglial dephosphorilation, however ADP degradation is strongly dependent on microglial activity. **B.** Same data as above normalized to control enzymatic activity .

3.4. Analysis of microglial phagocytic activity

According to our previous results (see section 3.3), ATP and ADP homeostasis in the brain is done by microglia using CD39. Whereas microglia in culture show a very good ability of dephosphorilating ATP, this action is shared to some extent with other ectoenymes in the brain tissue. Here microglia seem to be rather the responsible for the final dephosphorylation of the ATP subproducts to AMP. Therefore, measuring phagocytic activity directly in brain slices seems to be a necessary step in order to known more precisely how ATP homeosthasis and microglia function are interconnected.

To this end, we established a method to measure the phagocytic properties of microglia in brain slices. First, we checked that microglia in acute cultures retain the phagocytic properties by using bioparticles of *E. coli* labeled with

the pHrhodo fluorescent indicator (see section 2.2.13). Later, we wished to have a reliable method to quantify the phagocytic activity. For that, we used green fluorescence latex beads instead of bioparticles, which are difficult to quantify.

3.4.1 Microglial phagocytic activity is preserved in acute brain slices

To confirm that microglial phagocytic activity was intact in brain slices, we used bioparticles of *E. coli* labeled with the pHrhodo fluorescent indicator (see section 2.2.13). The recognition of the *E. coli* as pathogens by the microglia causes the engulfment of the particle inside phagosomes. Here the pH changes towards acidic values, which produces a conformational change in the pHrhodo molecule that provokes the emission of a intense red fluorescence upon excitation. In our experimental conditions, after incubation of pHrodo *E. coli* in acute brain slices of adult CX3CR1$^{+/-}$-eGFP mouse, red fluorescence particles was exclusively localized in microglia, thus proving that microglia retains intact the phagocytic activity in acute brain slices (Fig. 3.4).

To quantify the phagocytic activity, we used green fluorescence latex beads. *In situ* phagocytosis assay was developed and performed as described in section 2.2.14. After incubation of the acute brain slices of adult mice with the fluorescence beads, many of them were internalized in the microglia. To verify whether the beads were inside the cell, we stained the preparation with Iba1 antibody and examined it using a laser scan microscope. Beads mostly localized in the somata and end feet protusions (Fig. 3.5b and 3.5a). Here we observed that some of the beads were clearly surrounded by microglial cytoplasm. However, the possibility that a portion of them were only partially engulfed could not be excluded. Another proportion of beads was clearly not attached to the microglial cells and mainly remained on the slice surface. Beads found in the immediate vicinity to astrocytic processes were in contact with the processes but not internalized (Fig. 3.5c). Therefore, only beads that were unequivocally identified inside the microglia were considered to be phagocytosed and used for quantification.

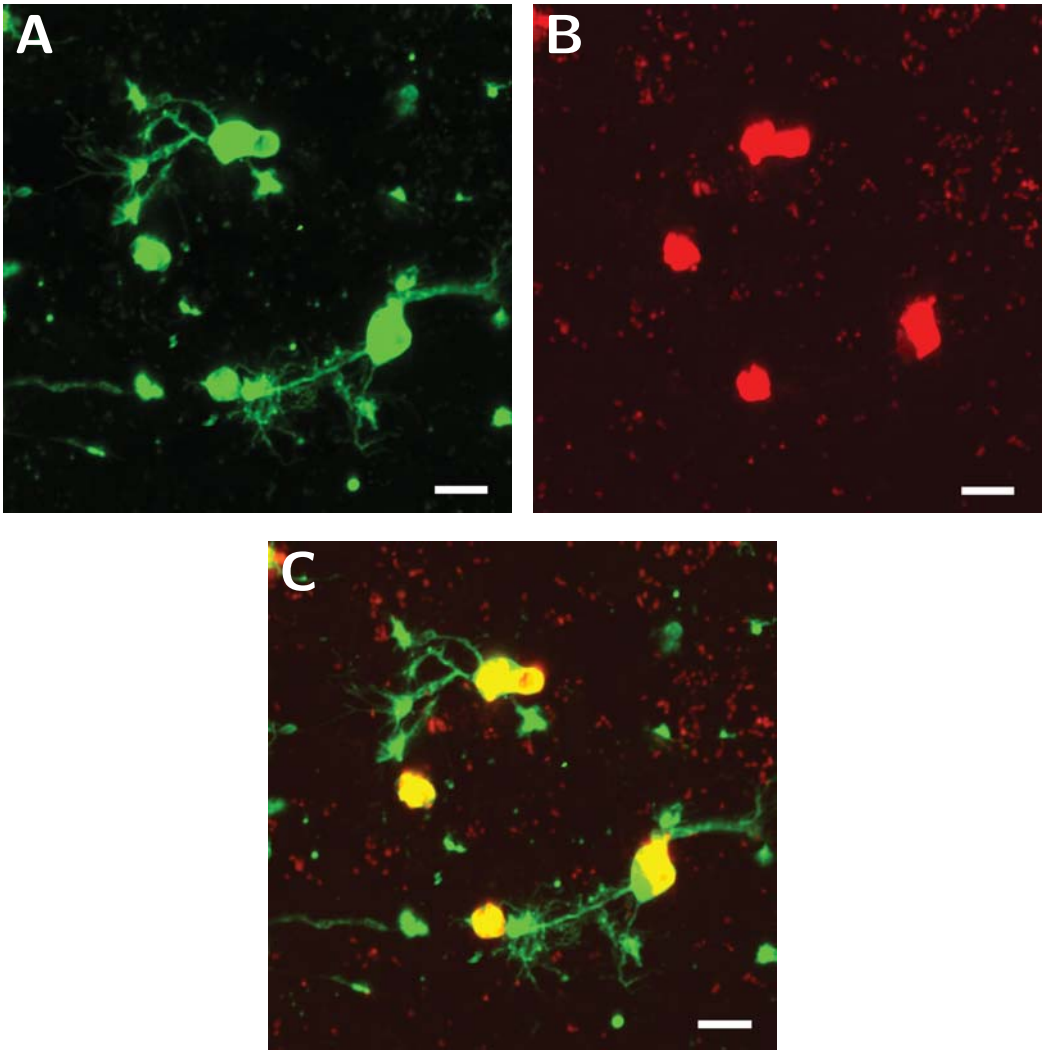

Figure 3.4 – Microglial phagocytosis of phRodo *E. coli* bioparticles.
Two-photon imaging of acute brain slices of adult CX3CR1$^{+/-}$-eGFP (green) mouse incubated with phRodo *E. coli* bioparticles (red). Scale bar, 15 µm. **A.** Ramified microglia from a typical brain slice from CX3CR1$^{+/-}$-eGFP mouse. **B.** phRodo *E. coli* bioparticles. Upon internalization in the microglia, fluorescence intensity was highly increased. **C.** Overlay picture showing that every highly fluorescence phRodo *E. coli* was within the microglia cell limits.

3.4.2 Phagocytosis of latex beads by microglia does not depend on pre-incubation time of acute brain slices

Since preparation of brain slices is *per se* a traumatic event, it is reasonable to think that it might cause the activation of microglia and that this would have an effect on its phagocytic activity. To observe the dynamic of such an effect, we quantified microglial phagocytic activity in acute brain slices at different

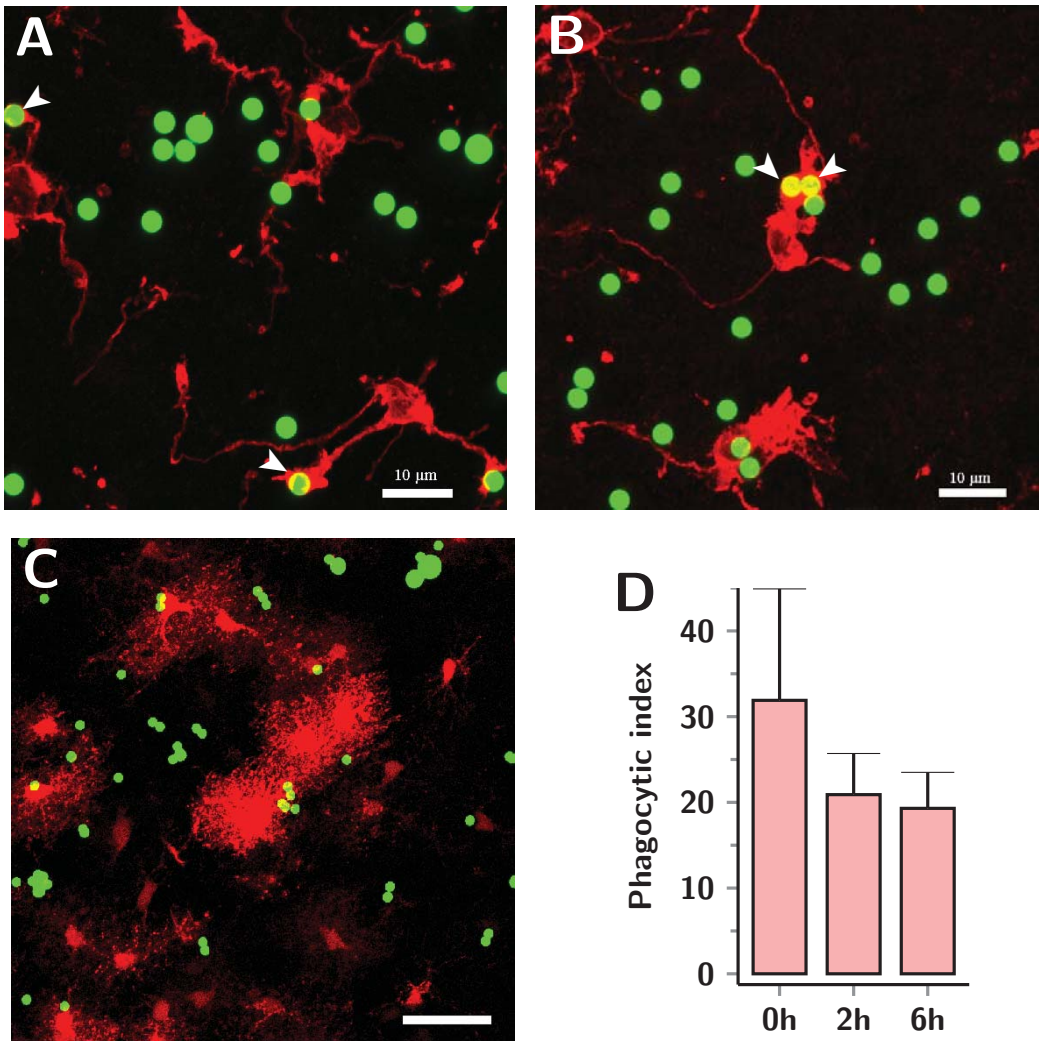

Figure 3.5 – Fluorescence latex beads are phagocytized only by microglia. Typical example of the *in situ* phagocytosis assay with opsonized latex microspheres. Green fluorescent latex beads were mostly adhered to the surface of the brain slice. Microglia as well as astrocytes were capable of making contacts to the beads. Phagocytozed beads were recognized by the spatial colocalization within the borders of the cell membrane. **A.** Example of beads inside Iba1-immunostained microglial end feet processes (arrow heads, ➤). Scale bar, 10 µm. **B.** Example of beads inside Iba1-immunostained microglial soma (arrow heads, ➤). Scale bar, 10 µm. **C.** Example of beads making adhesive contacts to RFP-expressing astrocytes. Scale bar, 30 µm. Opposite to microglia, astrocytes were not able to internalize the beads. **D.** Phagocytosis of latex beads by microglia does not depend on pre-incubation time of acute brain slices. Acute slices of control animals were kept in ACSF medium for 0, 2 or 6 h before opsonized latex beads were applied. Phagocytic index of microglia for each time point was calculated. No significant difference among the groups was found.

time points. Thus, fluorescence latex beads were added to the brain slice either at 0 h (immediately after the preparation), after 2 h or after 6 h. Phagocytic

activity was quantified as previously described (see section 2.2.13). Here we found no significant differences between the different time points (Fig. 3.5d). A morphological shift from ramified to ameboid microglia was also not observed.

Therefore, we arbitrarily chose to perform all the further experiments at time point equals to 2 h for practical reasons.

3.4.3 MCAO increases microglial phagocytosis

To verify the reliability of the newly developed phagocitic assay, we used the well-studied model of MCAO. In agreement with previous studies (Schilling et al., 2005), a dramatic and significant phagocytosis increase was observed in the ipsilateral hemisphere, validating therefore the assay. On average, in the injured side there were 125.9 ± 5.7 beads/100×cell (n=4) while in the control side, we observed only 19.8 ± 5.9 beads/100×cell (n=4) (***) (Fig. 3.6). Iba1-immunostaining showed that the microglia in the lesioned hemisphere exhibited a highly activated morphology. Here, it could be argued that these cells could be peripheral monocytes, which entered the brain through the disrupted brain-blood-barrier (BBB). However, previous results (Schilling et al., 2005) showed that hematogenous macrophages invaded the ischemic area not earlier than on day 4 and it is indeed the resident microglia cells, who are responsible for the phagocytosis at the lesion site.

3.5. Dependence of microglial phagocytic activity on CD39 expression

Our previous results showed that microglia is able to control the ATP level by a CD39-dephosphorylation mechanism. However, in bran slices, homeostatic control of ATP by microglia through CD39 was partially compensated. Therefore, we questioned next whether *cd39*-deficiency would influence the phagocytic function of microglia or, on the other hand, these brain compensatory mechanisms are sufficient to keep the microglial phagocytosis unchanged.

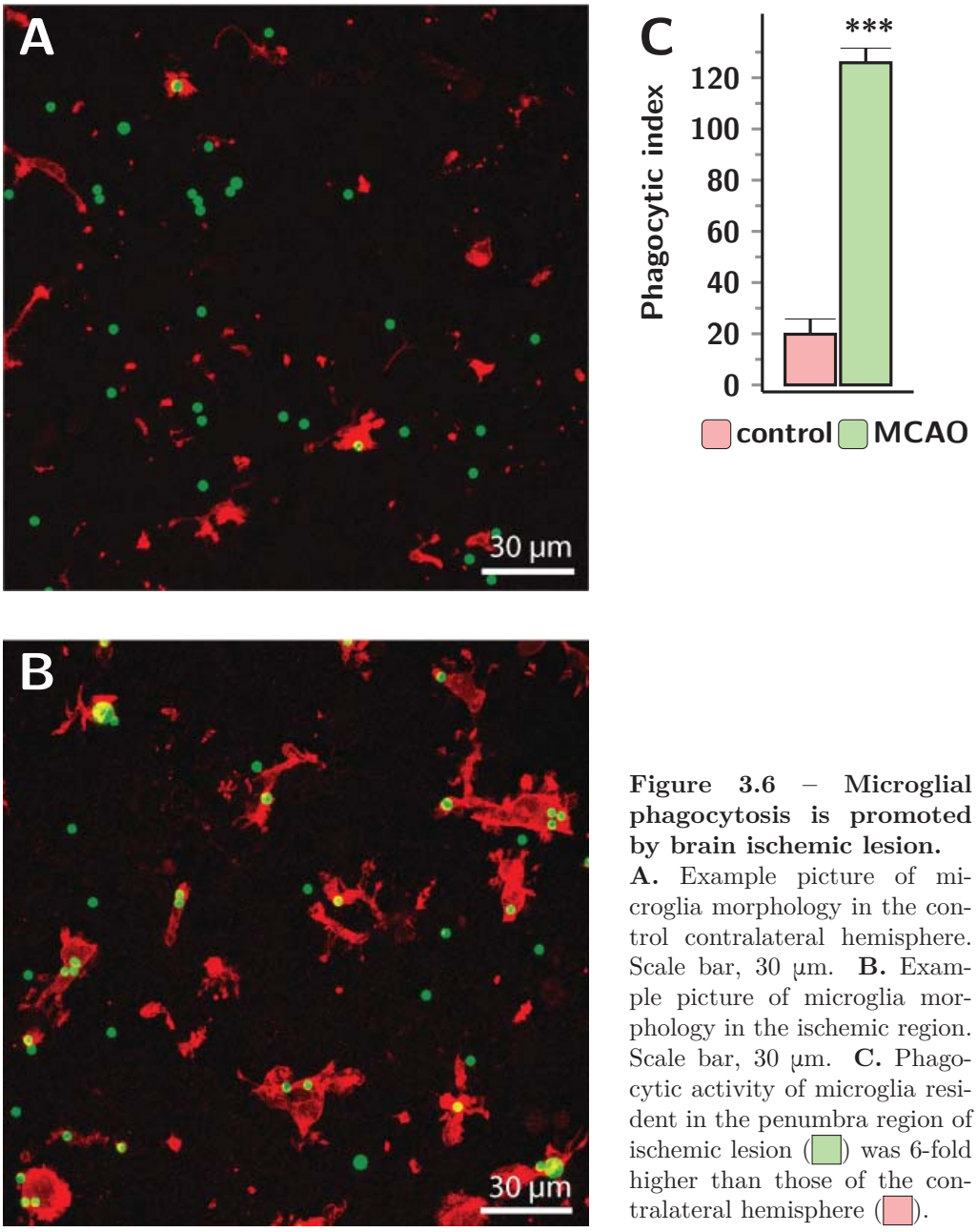

Figure 3.6 – Microglial phagocytosis is promoted by brain ischemic lesion. **A.** Example picture of microglia morphology in the control contralateral hemisphere. Scale bar, 30 µm. **B.** Example picture of microglia morphology in the ischemic region. Scale bar, 30 µm. **C.** Phagocytic activity of microglia resident in the penumbra region of ischemic lesion ( ) was 6-fold higher than those of the contralateral hemisphere ( ).

3.5.1 CD39 deficiency leads to increased phagocytic activity of microglia

For that, we examined acute brain slices in *cd39* deficient mice and wild type animals using the *in situ* phagocytosis assay described above (see section 2.2.13). The results revealed a significant elevation of phagocytic ac-

tivity in absence of *cd39*. While the phagocytic index in *cd39*$^{-/-}$ was 73.6 ± 10.4 beads/100×cell (n=10), in control animals it was only 24.6 ± 4.75 beads/100×cell (n=10) (***), with *n* representing the number of brain slices used for analysis (Fig. 3.7a).

Application of 100 µM ATP during the assay led consequently to increased phagocytosis in wild type animals: 189 ± 15 % (n=7) compared to untreated slices (***) (Fig. 3.8a). Interestingly, ATP did not cause a significant increase of phagocytosis in absence of *cd39* (117 ± 11 % (n=7) compared to untreated *cd39*$^{-/-}$ slices). This result would indicate that the phagocytic machinery in *cd39*$^{-/-}$ microglia is saturated and/or that *cd39* is responsible for the phagocytic potentiation by ATP.

3.5.2 Ameboid microglia from young animals exhibit higher phagocytic activity

Already Del Río Hortega described in his first works that the morphology of microglia changes during development (Del Río Hortega, 1932). Whereas young mice present a high population of ameboid cells, ramified microglia is the main type present in adult animals. Furthermore, ameboid microglia is most likely to migrate to the surface of acute brain slices of young animals and perform phagocytic removal of dead and damaged cells there (Brockhaus et al., 1996). To know whether microglia phagocytic ability changes during development as well, we examined the phagocytic activity of microglia in acute brain slices from adult and young mice.

Here we found that, indeed, the microglia from P6-P9 animals showed a significantly higher phagocytic activity than the one of adult animals, namely we calculated 136.5 ± 13.5 beads/100×cell (n=6) in the young animals and 24.6 ± 4.7 beads/100×cell (n=10) in adult mice (***) (Fig. 3.7a). Microglia from P6-P9 animals is known to be ameboid, whereas the one of adult animals is ramified (Del Río Hortega, 1932). In fact, this is the phenotype that we found as well during our experiments (Fig. 3.7b and 3.7d). This could mean that the mechanisms that regulate phagocytosis in ramified microglia are different from those of ameboid microglia. This increased level of phagocytic activity is justified by ongoing processes of brain development at this age and must be of non-inflammatory nature.

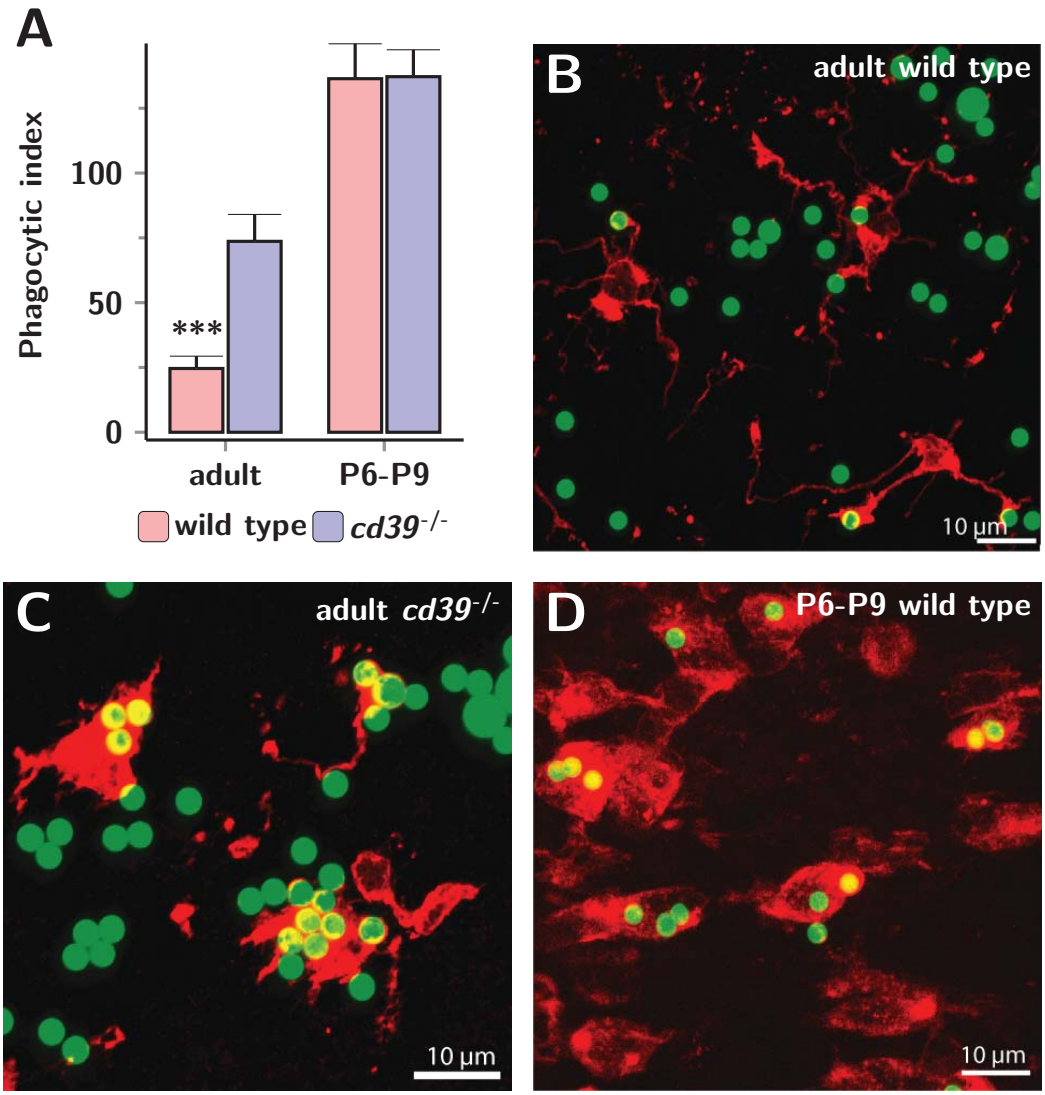

Figure 3.7 – CD39 deficiency increases phagocytosis.
A. Comparison of the phagocytic index of microglia from control ( ) and *cd39*$^{-/-}$ mice in young and adult animals ( ). Microglia is low phagocytic in adult animals, however *cd39*-depleted microglia exhibited a higher phagocytosis. Microglia from young animals was, on the other hand, highly phagocytic and activity was similar to *cd39*-depleted pups. **B.** Example picture of microglia from an adult wildtype brain slice. Scale bar 10 µm. **C.** Example picture of microglia from an adult *cd39*$^{-/-}$ brain slice. In adult mice from both genetical backgrounds, microglia was ramified. Scale bar 10 µm. **D.** Example picture of microglia from a young wildtype brain slice. Here microglia showed an ameboid phenotype. Scale bar 10 µm.

3.5.3 Control of microglial phagocytic activity in young animals does not require CD39

From our previous experiments we know that, indeed, ATP homeostasis regulates microglia phagocytosis from adult brain through a CD39-dependent

mechanism. Therefore, we wanted to see next if this was the case in young brain as well.

When we compared the microglial phagocytic activity *in situ* of wild type and CD39-deficient adult animals, we found that phagocytosis in absence of CD39 was about three times bigger, namely, the phagocytic index of microglia from knockout mice was 73.65 ± 10.38 beads/100×cell (n=10) and in wild type animals was only 24.6 ± 4.75 beads/100×cell (n=10) (***). The phagocytic index of microglia from pups of *cd39*$^{-/-}$ mice was unchanged in comparison to wild type animals, namely, 137.2 ± 10.4 (n=6) and 136.4 ± 13.5 beads/100×cell (n=6) (***), respectively.

According to these results, phagocytosis in young ameboid microglia is CD39-independent. These results brings new and interesting questions about how phagocytosis is controlled in young animals. If phagocytosis is still regulated by ATP homeostasis as in the adult brain, an alternative mechanism different from CD39-dependent dephosphorylation of the extracellular ATP levels in parenchyma should be present.

3.6. Microglial phagocytosis is counterbalanced by two different purinergic inputs

So far, the present work indicates that phagocytic activity of microglia is promoted in absence of *cd39*. Lack of this phosphohydrolase would lead to ATP and ADP accumulation, since the main pathway of ATP dephosphorylation to AMP in the brain is missing. We showed furthermore that increase of extracellular ATP concentration causes increased microglial phagocytic activity. Next, we examined the action mechanism of this process.

3.6.1 Blocking of P2 receptor activation greatly impaired CD39-dependent microglial phagocytic function

As described in section 1.3, microglia function is believed to be regulated by a combined action of the two kinds of purinergic receptors, P1 and P2. We used the broad spectrum P2-purinoreceptor blocker PPADS (pyridoxal-5'-phosphate-6-azophenyl-2,4-disulfonate, see section 2.2.16) to examine the importance of purinergic activation in phagocytosis of microglia. When 100

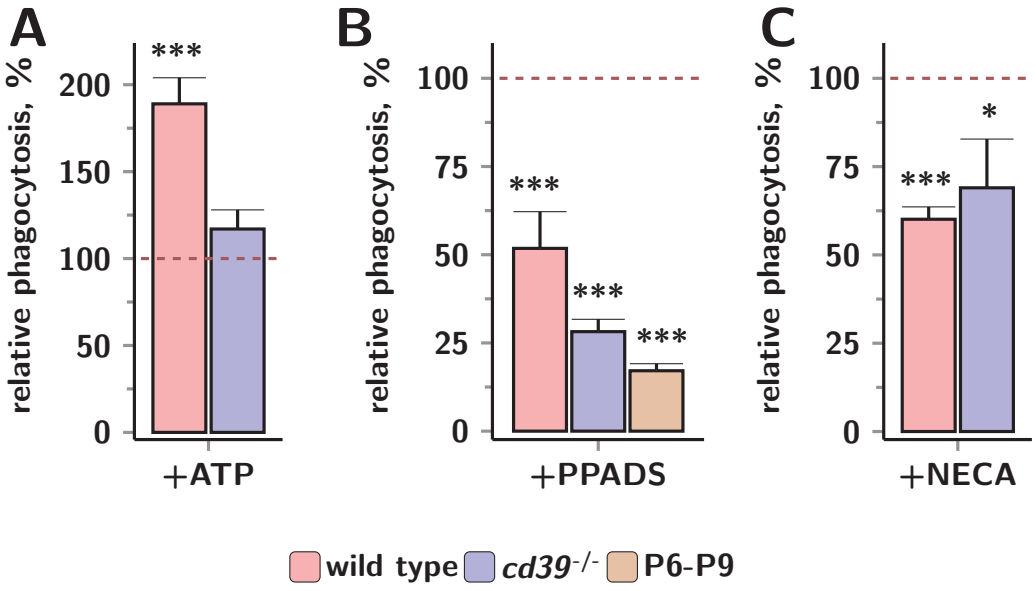

Figure 3.8 – P1 and P2 purinoreceptors are involved in regulation of microglial phagocytosis.
A. Application of ATP highly increased microglial phagocytosis in control animals ( ) in comparison to basal phagocytosis but not in *cd39*$^{-/-}$ mice ( ). **B.** Pharmacological blockage of P2 purinoreceptors by non-specific P2 blocker PPADS (100 µM) significantly decreased microglial phagocytosis in brain slices from control (adult and P6-P9 mice) and *cd39*$^{-/-}$ adult mice. **C.** Activation of P1 receptors by non-hydrolysable adenosine analog NECA (10 µM) also decreased phagocytosis in brain slices from wildtype and *cd39*$^{-/-}$ animals.

µM PPADS was added, microglial phagocytic activity was significantly reduced in both wild type and *cd39*$^{-/-}$ slices as compared to control conditions. Thus, PPADS produced a decrease in phagocytic activity in wild type animals from 24.5 ± 1.2 (n=4) to 12.7 ± 1.2 beads/100×cell (n=4) (***). In CD39-deficient animals, the decrease caused by PPADS application was from 47.0 ± 2.9 (n=4) to 13.2 ± 0.9 beads/100×cell (n=4) (***). Threfore, when normalized to the phagocytic activity measured in non-treated controls, phagocytosis in wild types decreased to 51.8 ± 10.4 % (n=4) and even more dramatically in absence of *cd39* (28.2 ± 3.5 % (n=4) (***), Fig. 3.8b).

3.6.2 Blocking P2 receptors with PPADS decreased microglial phagocytic activity in P6-P9 WT animals

Treatment of P6-P9 acute brain slices from wild type animals with 100 µM PPADS caused consequently a significant decrease in microglia phagocytic activity. Here, we observed a nearly six fold reduction of phagocytic activity

in PPADS-treated slices (24.2 ± 2.8 beads/100×cell (n=3)) when compared to untreated slices (141.5 ± 8.7 beads/100×cell (n=3), ***).

3.6.3 Activation of P1 receptors by non-hydrolysable analog of adenosine decreased microglial phagocytosis

In addition to the well established activation of phagocytosis through P2 receptor signaling, we tested whether P1 receptor activation can influence this function in microglia. We tested for the involvement of P1 receptors by activating the receptors with the non-hydrolysable analog of adenosine, (1-(6-amino-9H-purin-9-yl)-1-deoxy-*N*-ethyl-β-D-ribofuran-uronamide, NECA 10 μM). The phagocytic activity was reduced in the presence of NECA to 60.1 ± 3.5 % (n=3) of control, ***(Fig. 3.8c). The same effect of NECA was observed in slices from *cd39*$^{-/-}$ animals, where phagocytosis decreased to 69.0 ± 13.8 % (n=3) of control (***).

In sight of the previous results, we identified P2 activation as the main factor that regulates phagocytic response in microglia. This leads to the following paradigm (Fig. 4.1) Phagocytosis in adult microglia is regulated by two opposite mechanisms. Whereas P2 activation produces a increase in the phagocytic response, P1 activation serves as a negative control. The dual purinergic input acts therefore to balance the phagocytic activity. Increased extracellular ATP, either by active cellular release as danger signal, by exposure of intracellular ATP during cellular death or by impairment of the CD39 enzymatic activity, would lead to increased P2 activation over the P1 inhibition and consequently increased phagocytic activity.

3.7. Influence of cd73 expression on AMP degradation and microglial phagocytosis

Increased extracellular ATP concentration would cause hypothetically an increase of AMP production, which via CD73, would be metabolized to adenosine causing the activation of P1 receptors and down-activation of phagocytosis. In this fashion, phagocytosis could be controlled and overactivation would be prevented. When we examined the dephosphorylation activity of *cd73*-deficient for ATP and ADP, we observed that this was unchanged in

comparison to wild type animals. The enzymatic activity for ATP in *cd73* $^{-/-}$ animals was 3.55 ± 0.52 µmol phosphate/mg protein/min (n=10) and 3.68 ± 0.36 µmol phosphate/mg protein/min (n=10) in the control group (Fig. 3.9a). ADP dephosphorylation was slightly yet significantly decreased in absence of *cd73*. In control conditions the enzymatic activity for ADP was 1.64 ± 0.12 and only 0.88 ± 0.13 µmol phosphate/mg protein/min in *cd73* $^{-/-}$ animals (53.6 ± 8.1 % of the control group, ***).

However, phosphate production from AMP by brain tissue from *cd73* $^{-/-}$ animals revealed a strong decrease compared to the activity of brain tissue from wild type animals (0.62 ± 0.04 (n=10) and 0.02 ± 0.01 µmol phosphate/mg protein/min (n=10) (***), Fig. 3.9a and 3.9b). Application of AMP to brain slices from wild type and *cd73* $^{-/-}$ animals showed therefore a strong impact of *cd73* for the degradation of AMP.

Suprisingly, we found no difference in phagocytic activity in wild type compared to *cd73* $^{-/-}$ microglia. Phagocytic indexes (39.7 ± 5.6 beads/100×cell (n=10) in wild type and 39.9 ± 3.7 beads/100×cell (n=10) in *cd73* $^{-/-}$) were not significantly different (Fig. 3.9c).

This result is in agreement with previous studies showing that the AMP produced by dephosphorylation of ATP and ADP is further degraded to adenosine by the extracellular ecto-nucleotidase CD73, which is the only extracellular enzyme with such activity known up to date (Zimmermann, 1992). It was further shown that TNAP might support 5'-nucleotidase in conditions that require more effective AMP hydrolysis and adenosine production (Kukulski et al., 2011). However, with this experiment we showed that there is no compensatory mechanism for the action of CD73 in microglia. Furthermore, an eventual accumulation of non-hydrolyzed AMP in *cd73* $^{-/-}$ tissue could, in turn, slow down the ADP hydrolysis.

To summarize, absence of CD73 causes, as expected, a decrease in the AMP dephosphorylation function of microglia, which would lead to a decreased extracellular adenosine concentration and decrease in the inhibition of phagocytosis by P1-activation. However, remarkably, phagocytic activity of microglia is preserved in CD73-deficient mice. This may suggest that, while increase of extracellular adenosine inhibits phagocytosis, decrease of adenosine concentration does not affect the basal level of phagocytic activity.

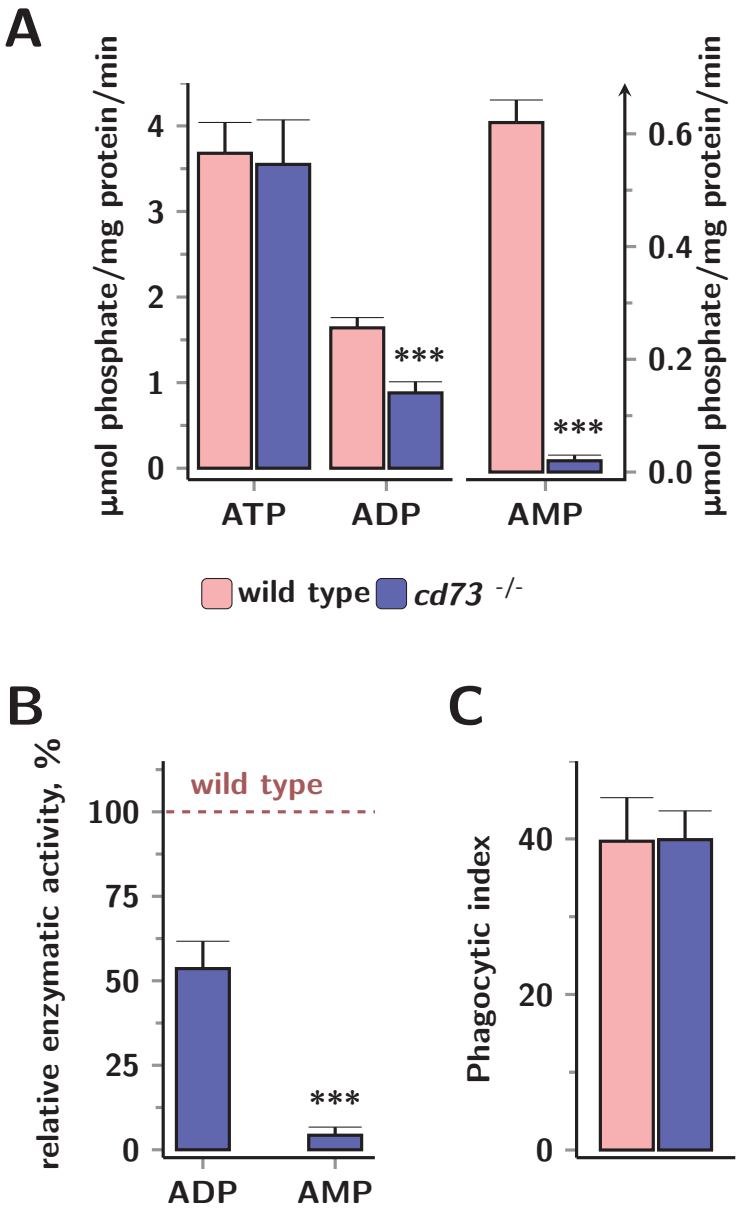

Figure 3.9 – Acute brain slices of CD73 KO mice are virtually incapable of extracellular AMP degradation as compared to WT.
A. Extracellular purines (1 mM ATP, ADP and AMP solutions) were cleaved in wild type acute slices ( ) and *cd73* $^{-/-}$ ( ) acute brain slices. Mean values of free orthophosphate release in µmol phosphate/mg protein/min were summarized from three independent experiments. Acute slices of *cd73* $^{-/-}$ degraded ADP and AMP significantly less efficient as compared to WT. **B.** WT acute slices enzymatic activity was considered as 100% for ADP and AMP degradation (at 100%). *cd73* $^{-/-}$ acute slices were far less potent in ADP degradation and virtually incapable of AMP cleavage as compared to wild type acute slices. **C.** Decreased production of extracellular adenosine in *cd73* $^{-/-}$ animals had no effect on microglia phagocytic activity.

CHAPTER 4

Discussion

4.1. Relevance of the work

Microglia is the largest population of the resident macrophages in the CNS. Even in a healthy CNS environment, microglia is very active (Nimmerjahn et al., 2005; Davalos et al., 2005; Wake et al., 2009). Under normal conditions, microglia presents a highly branched phenotype with long processes that survey constantly the local region of parenchyma. Microglia cells are often referred as sensors of pathology (Hanisch and Kettenmann, 2007), since any disbalance of the CNS homeostasis leads to a rapid activation of microglia, changing its morphology and the cell-surface antigen expression. Activated microglia retract the processes to acquire an ameboid morphology. Depending on the nature of the activating stimuli, microglia can produce pro-inflammatory (by releasing pro-inflammatory mediators and activating phagocytosis) or anti-inflammatory response (by removing apoptotic cells and myelin debris) (Hanisch et al., 2001; Häusler et al., 2002).

Microglia is an active player during brain development by having an role in shaping brain architecture. Programmed cell death (PCD) of neural cells promotes non-inflamatory microglia phagocytosis. Microglia participates here in clearance of dead cells and has therefore a very important anti-inflammatory effect. However, microglia also engulfs still-living neural cells and axons, controlling axon pruning (Mallat et al., 2005).

In the adult brain, microglia plays an important role during the innate inflammatory response. Animal models of acute brain injury indicated that microglia activity exacerbates the lesion size and is detrimental for neurological outcome (Allan and Rothwell, 2003). During the period following to the initial lesions, there is an anterograde Wallerian degeneration of the damaged neurons as well as a retrograde degeneration of the neurons connected to them. Microglia participates here in the formation of anti-inflammatory (alternative activated) foam cells, which are responsible for the removal of degenerating axons and myelin.

Furthermore, microglia has a very important role in neuropathological conditions. The presence of activated microglia was documented in many animal models of brain diseases and in equivalent conditions in humans, such as Parkinson disease (PD), multiple sclerosis (MS), amyotrophic lateral sclerosis (ALS) and prion disease (Perry et al., 2010). In patients with Alzheimer disease (AD), PET imaging of activated microglia showed a inverse correlation in the amount of activated microglia with cognitive functions: as cognitive function declined over time, the ^{11}C-R-PK11195 signal originated in activated microglia increased (Banati, 2002). Several studies have examined how promotion of microglia phagocytosis may delay the progress of amyloid plaques in AD. Different approaches have been used for that, including delivery of the LPS directly into the brain (Morgan et al., 2005), whole-body irradiation followed by bone marrow transplantation (Simard et al., 2006), and systemic injection of macrophage colony stimulating factor 1 (M-CSF) (Boissonneault et al., 2009). From all, the most promising approach seems to be boosting microglia phagocytosis in AD by immunization with Aβ or delivery of specific anti-Aβ antibodies (Schenk et al., 1999). Thus, microglia phagocytosis in brain inflammatory response must play a tremendous role in delaying the disease progression.

One of the recently discovered, and therefore not completely understood yet, mechanism for the regulation of microglial phagocytosis is the regulation by the purinergic system. Up to today, it is believed that activation of $P2Y_6$ receptor by extracellular UDP leads to an increase of microglial phagocytosis *in vitro* as well as *in vivo* (Koizumi et al., 2007). One additional study showed that *in vitro* short-term exposure of microglia to high concentrations of ATP (1 mM) induced attenuation of phagocytosis through $P2X_7$ receptor activation

(Fang et al., 2009). Additionally, activation of adenosine receptors (A_{2A} or A_{2B}) was shown already in classic studies to have suppressive effect on cultured monocytes phagocytosis as well as on macrophages (Leonard et al., 1978). Interestingly, in freshly isolated undifferentiated monocytes, the A_1 receptor agonist CPA was capable of enhancing phagocytosis, indicating a role of A_1 receptors in promoting Fcγ-receptor-mediated phagocytosis (Salmon et al., 1993).

Taken together, both P1 and P2 receptors seem to play a role in the regulation of phagocytosis in monocytes, macrophages and microglia. This work pursed, therefore, to investigate the interconnection between microglia function and purinergic homeosthasis. To this end, we examined (1) how microglia is involved in the buffering of the purinergic ligands in the CNS and (2) how changes in these signals may affect microglia phagocytic function.

4.2. Role of microglia in the buffering of purinergic ligands in the CNS

Accessibility of ligands for purinergic receptors – nucleoside tri- and diphosphates – depends on the balance between their release from cells and enzymatic degradation (Kukulski et al., 2011). Enzymes responsible for degradation differ in their kinetic properties and expression patterns among different cell types. E-NTPDase1 (CD39) is the ecto-enzyme specifically expressed by microglia in the brain parenchyma (Murabe and Sano, 1982) and is responsible for the high ATP/ADP degradation capacity of these cells.

Comparison of the activity of purine-phosphate degrading extracellular enzymes in purified cell cultures of astrocytes and microglia showed that microglia have an about 3-fold higher ATP-degrading activity as compared to astrocytes. Moreover, ADP degradation by microglia was even 5-fold higher as those in astrocytes. This is due to the fact, that E-NTPDase2, expressed by astrocytes, is obviously less efficient in ATP and, especially, ADP hydrolysis as compared to microglia-specific CD39. While microglial E-NTPDase1 can equally well convert ATP and ADP to AMP, astrocytic E-NTPdase2 is rather inefficient for metabolizing ADP (Robson et al., 2006).

CD39 is responsible for nearly all ATP/ADP degrading activity in cul-

tured microglia as revealed by comparison of specific enzymatic activities in microglial cultures from wild type and *cd39*-deficient animals. Generation of free phosphate from ATP and ADP was virtually absent in *cd39*$^{-/-}$ microglial cultures, indicating that CD39 is the major enzymatic component of microglia for the ATP and ADP degradation.

In the brain tissue, extracellular ADP removal is mainly done by a CD39-dependent dephosphorylation. We showed that only the ADP-, but not the ATP-degrading activity was affected in the brain slices of *cd39*-deficient animals. This observation reflects the redundancy of ATP- (and not ADP-) converting extracellular enzymes in the brain tissue. Indeed, NTPDases-2,3,8, E-NPP family and alkaline and acid phosphatases can all participate in efficient ATP removal, while microglia-specific CD39 remains crucial for ADP hydrolysis. Because ADP (similarly to ATP and other purines) can be released into the extracellular space upon trauma or damage, it is important that microglia is capable to remove the excess of this danger molecule via its functional E-NTPDase1.

Another unique, non-redundant, enzyme, expressed inside the CNS mainly by microglia, is CD73, or 5'-nucleotidase. CD73 is responsible of converting AMP into the adenosine, thereby generating P1 receptors agonist. In the brain tissue of *cd73*-deficient animals, AMP hydrolysis into adenosine is disrupted. Moreover, the enzymatic activity of ADP degradation by CD39 was twice reduced in *cd73*-deficient animals, indicating that accumulation of AMP can in turn decrease the activity of CD39. It is known, that in the cases of severe adenosine lack, TNAP may support 5'-nucleotides in AMP hydrolysis and adenosine generation (Kukulski et al., 2011). However, in this particular experiment we did not observe any compensatory mechanism for the action of CD73. Never the less, it is possible, that in intact brain tissue the basal level of adenosine might be kept preserved due to TNAP or equilibrative nucleoside transporters (ENT), which can directly release intracellular adenosine into extracellular space (Parkinson et al., 2011).

Thus, microglia play a unique role in the purinergic homeostasis in the brain. Two of its ectoenzymes – CD39 and CD73 – are the major providers of purinergic receptors agonists. The absence of either of them leads to the severe disbalance of extracellular purines *in vivo* and *in situ*. To learn more about how redundant is the role of CD39 and CD73 in mouse brain, as well

as how purinergic homeostasis influences microglial phagocytic functions, we utilized a newly developed *in situ* phagocytosis assay.

4.3. Establishing of the in situ phagocytosis assay

The majority of phagocytosis studies in microglia were performed with cell cultures (von Zahn et al., 1997; Beletskii et al., 2005; Fang et al., 2009), where cells were removed from their natural tissue environment, often treated with growth factors to increase cell yields. Such treatment can irrevocably change cell phenotype and therefore a generalization of the obtained results to the microglia in tissue surroundings should be treated with caution. On the other hand, *in vivo* studies, where fluorescent particles were injected in the tissue and phagocytosis was evaluated using morphological methods, are difficult to perform (Hughes et al., 2010). We have, therefore, developed for the first time a method to quantify microglia phagocytic activity in acute brain slices. We first confirmed that microglial phagocytosis is preserved in this model by using the *E. coli* bioparticles labelled with a pH-sensitive fluorescent indicator. In our experimental conditions, red fluorescent signal from this bioparticles was intense and it exclusively localized in microglia, thus proving that microglia retains its phagocytic activity after acute brain slice preparation.

Next, we used opsonized fluorescent latex beads in order to enable quantitative approach. To verify the internal localization of beads, we used laser scanning confocal microscopy. Here we noticed that many of the fluorescent beads were attached to the surface of the slice. Only beads surrounded by microglial cytoplasm were considered to be phagocytosed and used for quantification. Yet, the possibility that a portion of the beads were only partially engulfed could not be excluded. However, a distinction between attachment and internalization of opsonized beads may not be critical, as several studies have shown in the past that phagocytic cells rapidly engulf microorganisms after the attachment step (Peterson et al., 1977; Kuypers et al., 1989; Martin and Bhakdi, 1991).

After testing the microglial phagocytic activity at different time points (immediately after the preparation, and 2h or 6h later) we did not observe a significant difference in microglial phagocytosis. Therefore, we have chosen 2h after the preparation as a time of phagocytosis onset (that is, adding beads to

slices) for practical reasons.

This method of phagocytic activity assessment was, to our knowledge, not utilized or published before. To verify its reliability, we quantified microglia phagocytosis in the brain tissue 48h after middle cerebral artery occlusion (MCAO). In agreement with already published data (Schilling et al., 2005), we observed a dramatic and significant increase of the microglial phagocytic activity in the ipsilateral hemisphere. We further utilized this assay to investigate how the purinergic system is involved in regulating microglial phagocytosis.

4.4. Microglia phagocytic activity is regulated by P2 purinergic receptors

According to our results, in the brain tissue of *cd39*-deficient animals, homeostatic control of ATP levels was partially compensated by other mechanisms, while ADP levels were still elevated. We next checked if an impaired ATP/ADP dephosphorylation would affect microglial phagocytic activity. Indeed, we observed a significant elevation (about 5-fold) of microglial phagocytosis in the absence of CD39. We assume that due to the lack of CD39 activity, the basal ATP/ADP level is elevated, which leads to a chronic stimulation of the microglial phagocytic activity. This is supported by the observation that (1) the blocker of P2 signaling, PPADS, reduced phagocytic activity in wild type and *cd39*-deficient slices to the basal low level and that (2) addition of ATP did not further increase phagocytic activity in *cd39*-deficient animals.

One could hypothesize that chronic elevated ADP levels in the brain tissue of *cd39*-deficient animals could cause global gene expression and functional changes of microglial cells during the organism development. Such changes would, in turn, cause elevated phagocytic activity of microglia, independent of P2 receptors expression. In other words, blockage of P2 receptors would be irrelevant to the phagocytic activity of microglia. However, the fact that short-term application of PPADS quickly returned the phagocytosis back to the low level, speaks against this hypothesis. Thus, we can conclude, that in the brain tissue of *cd39*-deficient animals with constantly elevated ADP levels, P2 receptors do not undergo desensitization or down-regulation; and even if they do, it is apparently not enough to return the increased phagocytic activity to its control levels. To further verify the extent of down-regulation and/or desen-

sitization of P2 receptors in *cd39*-deficient mice, qPCR and pharmacological experiments would be required.

We next investigated how P2 receptors may influence microglial phagocytosis during the organism development. We found that in P6-P9 wild type pups microglial phagocytosis is at least 2-folds higher than in adults. This increased level of phagocytic activity in young pups is justified by the ongoing processes of brain development and must be of non-inflammatory nature. Interestingly, in *cd39*-deficient P6-P9 pups, microglia phagocytic activity was unchanged as compared to wild type pups. A possible explanation for this finding is that, in young animals, basal microglial phagocytosis is saturated and, consequently, an overactivation of phagocytic function by elevation of extracellular ATP/ADP concentrations due to the absence of CD39 cannot produce a further increase. This raises the new question of how the phagocytosis is regulated in young animals with brain still under development. It is possible that this type of phagocytosis is *cd39*-independent or even P2-receptors independent. However, blocking P2 receptors of P6-P9 animals with PPADS, led to a significant decrease of microglial phagocytosis, supporting, at least to some extent, the input of P2 receptors into the phagocytic activity of the ameboid microglia. It would be therefore very interesting to investigate the extracellular purine concentration in the living brain of young animals in comparison with adults.

4.5. Microglia phagocytosis is counterbalanced by two different purinergic inputs

In agreement with reported for microglial migratory activity (Färber et al., 2008), NECA led to a moderate inhibition of microglial phagocytic activity. Previously, similar mechanism, namely negatively regulated phagocytosis by P1 receptors stimulation, was described for mice macrophages and neutrophils (Haskó et al., 2007).

However, we did not observe any increase of microglial phagocytic activity in the tissue of *cd73*-deficient animals, even though AMP conversion to adenosine is drastically reduced. This discrepancy can be explained if (1) low adenosine concentrations (as opposed to increased concentrations) do not influence microglial phagocytic activity or (2) the basal level of adenosine is

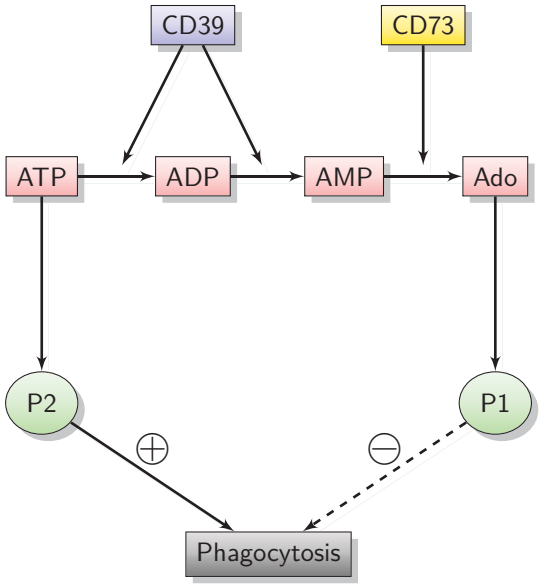

Figure 4.1 – Regulation of microglial phagocytosis through control of the ATP homeostasis.
According to the results, microglial phagocytosis might have a dual purinergic regulation. Whereas P2-activation by ATP produces a increase in phagocytic activity, P1-activation by Adenosine (Ado) causes a decrease in phagocytosis. Microglia might regulate the activation level by controlling the ATP homeostasis. Here CD39 would promote the degradation of ATP to AMP from the tissue environment, reducing P2-activation. In parallel, excess of AMP is dephosphorilated by CD73 into adenosine. This adenosine would activate P1 causing a downregulation of phagocytic activity.

kept preserved in *cd73*-deficient animals due to TNAP or equilibrative nucleoside transporters (ENT). The best experiment to prove this hypothesis would be microdialysis of *cd73*-deficient living animals' brain and consequent HPLC analysis of adenosine concentration. Altogether, we conclude that microglia play an exclusive role in purinergic homeostasis. Increased ATP concentration would normally cause an increased AMP production by microglia. Via CD73, AMP would be metabolized to adenosine, causing the activation of P1 receptors and down-regulation of increased phagocytosis. In this fashion, phagocytosis could be controlled and over-activation would be prevented (Fig. 4.1).

4.6. Further project directions

While the newly developed phagocytosis assay, utilized in this work, is sensitive enough to give physiologically significant results, further improvements can be done. It can benefit, for example, from developing a system with cul-

tured brain slices, where other cell types are preserved and microglia is kept in its resting state.

To directly measure the purinergic disbalance in the brain tissue of *cd39*- and *cd73*-deficient animals as well as to compare purine concentration in young and adult animals, ATP-microelectrodes, implanted in the brain of living animals, can be utilized. Microdialysis with subsequential HPLC is yet another alternative.

qPCR of microglia, freshly isolated from *cd39*- and *cd73*-deficient animals, can show the level of expression of P1 and P2 receptors. More pharmacological experiments with acute brain slices are needed to identify, which particular P2 receptors are involved in increased phagocytic activity of *cd39*$^{-/-}$ animals and if any desensitization takes place due to the chronic ADP elevation.

With the newly established in our laboratory system of two-photon *in vivo* imaging, we can now directly record the phagocytic events inside the brain tissue upon the microinjection of fluorescent beads or *E. coli* bioparticles. This will allow us to see how the purinergic balance influences the migration and phagocytosis of microglia upon the acute microinjury from the micropipette. Some preliminary data from our research already indicated that microglial processes movement towards the laser lesion is diminished in *cd39*-deficient animals.

Elevated phagocytic activity in *cd39*-deficient animals can be beneficial in some pathological conditions. Therefore, it can be interesting to check whether the senile plaques can be removed more efficient in *cd39*-deficient animals, subjected to Alzheimer disease. Prion disease is yet excellent another candidate to test, where increased microglial phagocytosis can be beneficial.

Altogether, the knowledge on regulation of microglial phagocytosis by purinergic system should help us in developing more efficient treatment for various neurodegenerative diseases.

Summary

Purinergic signaling plays a major role in the regulation of phagocytosis in microglia. Interplay between P2 and P1 receptor activation is controlled by a cascade of extracellular enzymes which dephosphorylate purines resulting in the formation of adenosine. The ATP and ADP degrading capacity of cultured microglia depends on the expression of E-NTPDase1 (CD39) and is several times higher when compared to astrocytes which lack this enzyme. In brain slices, deletion of *cd39* resulted in a 50 % decrease of ADP-degrading ability, while the degradation of ATP was decreased to about 75 % of the values measured in wild-type brain tissue. Microglia in acute slices from *cd39*$^{-/-}$ animals had increased constitutive phagocytic activity which could not be further enhanced by ATP in contrast to control animals. Pharmacological blockage of P2 receptors decreased the constitutive phagocytic activity to a similar base level in wild type and *cd39*$^{-/-}$ microglia. Activation of P1 receptors by non-hydrolysable adenosine analog significantly decreased phagocytic activity. Deletion of *cd73*, an enzyme expressed by microglia which converts AMP to adenosine did not affect phagocytic activity. Taken together, these data show that CD39 plays a prominent role in controlling ATP levels and thereby microglial phagocytosis.

Zusammenfassung

Purinerge Signaltransduktion spielt eine wichtige Rolle für die Phagozytoseaktivität von Mikrogliazellen. Das Zusammenspiel von P2- und P1-Rezeptoraktivierung wird durch eine Kaskade von extrazellulären Enzymen bestimmt, die Purine, wie ATP und ADP, bis hin zu Adenosin dephosphorylieren können. Mikroglia sind aufgrund der Expression der E-NTPDase1 (CD39) in der Lage weitaus mehr ATP und ADP abzubauen als beispielsweise Astrozyten, denen dieses Enzym fehlt. In Hirnschnitten CD39 defizienter Mäuse, konnte im Vergleich zu Kontrollschnitten sowohl eine auf 50% reduzierte ADP-Abbaurate als auch eine auf 75% verminderte ATP-Abbaurate gemessen werden. Mikrogliazellen in akuten Hirnschnitten CD39 defizienter Mäuse zeigen verglichen mit Kontrolltieren eine erhöhte basale Phagozytoseaktivität, die im Gegensatz zu Kontrollschnitten nicht weiter durch ATP Stimulation gesteigert werden kann. Durch Zugabe von P2 Inhibitoren konnte die konstitutiv erhöhte Phagozytoseaktivität von Mikroglialzellen in *cd39*$^{-/-}$ Hirnschnitten auf Wildtypniveau reduziert werden. Ebenso P1-Aktivierung mithilfe eines nicht-hydrolysierbaren Adenosinanalogs zeigte diesen Effekt. Im Gegensatz dazu hatte das Fehlen einer weiteren mikrogliaspezifischen E-NTPDase CD73, die den Abbau von AMP zu Adenosin vermittelt, keinen Effekt auf die Phagozytoseaktivität.

Zusammengefasst zeigen die Ergebnisse, dass CD39 eine bedeutende Rolle in der ATP Homöostase spielt und somit einen wichtigen Einfluss auf die Phagozytoseaktivität von Mikrogliazellen ausübt.

Selbstständige Erklärung

Ich, Larisa Bulavina , erkläre, dass ich die vorgelegte Dissertation mit dem Thema: “Roles of E-NTPDase1 (CD39) and 5’-eNT (CD73) enzymes in the regulation of microglial phagocytosis” selbst verfasst und keine anderen als die angegebenen Quellen und Hilfsmittel benutzt, ohne die (unzulässige) Hilfe Dritter verfasst und auch in Teilen keine Kopien anderer Arbeiten dargestellt habe.

Berlin, den 26. September 2012,

Larisa Bulavina

Acknowledgments

I would like to thank first of all Professor Helmut Kettenmann for giving me the possibility of doing this doctoral work in the department of Cellular Neuroscience of the Max-Delbrück-Center, as well as for his supervision and constant support.

My special acknowledgment to Dr. Vitali Matyash for his tireless supervision in the project and optimism during the length of my PhD. Furthermore, I thank Dr. Katrin Färber for the supervision in the initial steps of the work in the lab and PD Rainer Grass, Dr. Christiane Nolte as well as Dr. Susanne Wolf for their helpful comments on my work.

I am grateful as well to the Medical Neuroscience Program of Charité that provided me the chance to enroll in the program and gave a possibility to participate in interesting workshops and courses.

I really appreciate the collaboration of Adriana Rocha, Frank Szulzewsky and Grietje Krabbe, who made an immense work in the paper as well. For the coworkers in the lab I have only best words, starting from the previous members Dr. Marta Maglione, Dr. Bruno Bennedetti, Dr. Daniel Reyes Haro, Dr. Stefani Seifert, Dr. Grietje Krabbe and Jitender Kumar. My colleagues created a great working atmosphere and it was a very joyful workplace. For that I want to thank Julia Parnis, Katyayni Vinnakota, Min-Chi Ku, Adriana Rocha, Kristin Stock, Maria Pannel and Petya Georgieva. My special thanks for the support and motivation to Professor Tatjana Pivneva.

I regret I couldn't get to know the new members well enough, apart from seldom social meetings: Feng Hu, Nadine Richter and Daniele Mattel. I wish you all the best in the future career, guys.

The technical members of the lab - Irene Haupt and Regina Pieske - were

always there to help me with experimental work. They were really great support. Birgit Jarchow was always there when I needed any administrative help. With her help any organisational issues were infinite smoother.

Last but not least, I want to thank my boyfriend, and now my husband, Ignacio. Without his help, support and motivation, this work would not be done. And thanks to all the friends I found in the institute. I was very glad of being there for four years.

Bibliography

Abbracchio, M. P., Burnstock, G., Verkhratsky, A. and Zimmermann, H. (2009). Purinergic signalling in the nervous system: an overview. Trends in neurosciences *32*, 19–29.

Allan, S. M. and Rothwell, N. J. (2003). Inflammation in central nervous system injury. Philosophical transactions of the Royal Society of London. Series B, Biological sciences *358*, 1669–77.

Banati, R. B. (2002). Visualising microglial activation in vivo. Glia *40*, 206–17.

Belcher, S. M., Zsarnovszky, A., Crawford, P. A., Hemani, H., Spurling, L. and Kirley, T. L. (2006). Immunolocalization of ecto-nucleoside triphosphate diphosphohydrolase 3 in rat brain: implications for modulation of multiple homeostatic systems including feeding and sleep-wake behaviors. Neuroscience *137*, 1331–1346.

Beletskii, A., Cooper, M., Sriraman, P., Chiriac, C., Zhao, L., Abbot, S. and Yu, L. (2005). High-throughput phagocytosis assay utilizing a pH-sensitive fluorescent dye. BioTechniques *39*, 894–7.

Boissonneault, V., Filali, M., Lessard, M., Relton, J., Wong, G. and Rivest, S. (2009). Powerful beneficial effects of macrophage colony-stimulating factor on beta-amyloid deposition and cognitive impairment in Alzheimer's disease. Brain : a journal of neurology *132*, 1078–92.

Braun, N., Sévigny, J., Robson, S. C., Enjyoji, K., Guckelberger, O., Hammer, K., Di Virgilio, F. and Zimmermann, H. (2000). Assignment of ecto-nucleoside triphosphate diphosphohydrolase-1/cd39 expression to microglia

and vasculature of the brain. European Journal of Neuroscience *12*, 4357–4366.

Brockhaus, J., Ilschner, S., Banati, R. B. and Kettenmann, H. (1993). Membrane properties of ameboid microglial cells in the corpus callosum slice from early postnatal mice. Journal of Neuroscience *13*, 4412–4421.

Brockhaus, J., Möller, T. and Kettenmann, H. (1996). Phagocytozing ameboid microglial cells studied in a mouse corpus callosum slice preparation. Glia *16*, 81–90.

Castrop, H., Huang, Y., Hashimoto, S., Mizel, D., Hansen, P., Theilig, F., Bachmann, S., Deng, C., Briggs, J. and Schnermann, J. (2004). Impairment of tubuloglomerular feedback regulation of GFR in ecto-5'-nucleotidase / CD73 - deficient mice. Journal of Clinical Investigation *114*, 634–642.

Chilingaryan, A., Chilingaryan, A. M. and Martin, G. G. (2006). The three-dimensional detection of microvasculatory bed in the brain of white rat Rattus norvegicus by a Ca2+-ATPase method. Brain Research *1070*, 131–138.

Colgan, S. P., Eltzschig, H. K., Eckle, T. and Thompson, L. F. (2006). Physiological roles for ecto-5'-nucleotidase (CD73). Purinergic Signalling *2*, 351–360.

Davalos, D., Grutzendler, J., Yang, G., Kim, J. V., Zuo, Y., Jung, S., Littman, D. R., Dustin, M. L. and Gan, W.-B. (2005). ATP mediates rapid microglial response to local brain injury in vivo. Nature neuroscience *8*, 752–8.

Del Río Hortega, P. (1932). Microglia. In Cytology and Cellular Pathology of the Nervous System, (Penfield, W., ed.), vol. 13, pp. 482–534. P. B. Hoeber, Inc. New York, NY.

Di Virgilio, F. (2005). Purinergic mechanism in the immune system: A signal of danger for dendritic cells. Purinergic signalling *1*, 205–9.

Endres, M., Laufs, U., Huang, Z., Nakamura, T., Huang, P., Moskowitz, M. A. and Liao, J. K. (1998). Stroke protection by 3-hydroxy-3-methylglutaryl (HMG)-CoA reductase inhibitors mediated by endothelial nitric oxide synthase. Proceedings of the National Academy of Sciences of the United States of America *95*, 8880–8885.

Enjyoji, K., Sévigny, J., Lin, Y., Frenette, P. S., Christie, P. D., Esch, J. S., Imai, M., Edelberg, J. M., Rayburn, H., Lech, M., Beeler, D. L., Csizmadia, E., Wagner, D. D., Robson, S. C. and Rosenberg, R. D. (1999). Targeted disruption of cd39/ATP diphosphohydrolase results in disordered hemostasis and thromboregulation. Nature medicine *5*, 1010–7.

Fang, K.-M., Yang, C.-S., Sun, S. H. and Tzeng, S.-F. (2009). Microglial phagocytosis attenuated by short-term exposure to exogenous ATP through P2X receptor action. Journal of neurochemistry *111*, 1225–37.

Färber, K., Markworth, S., Pannasch, U., Nolte, C., Prinz, V., Kronenberg, G., Gertz, K., Endres, M., Bechmann, I., Enjyoji, K., Robson, S. C. and Kettenmann, H. (2008). The ectonucleotidase cd39/ENTPDase1 modulates purinergic-mediated microglial migration. Glia *56*, 331–41.

Fiebich, B. L., Biber, K., Lieb, K., Van Calker, D., Berger, M., Bauer, J. and Gebicke-Haerter, P. J. (1996). Cyclooxygenase-2 expression in rat microglia is induced by adenosine A2a-receptors. Glia *18*, 152–60.

Fujita, S. and Kitamura, T. (1975). Origin of brain macrophages and the nature of the so-called microglia. Acta neuropathologica Supplementum *Suppl 6*, 291–296.

Garavaglia, S., Bruzzone, S., Cassani, C., Canella, L., Allegrone, G., Sturla, L., Mannino, E., Millo, E., De Flora, A. and Rizzi, M. (2012). The high-resolution crystal structure of periplasmic Haemophilus influenzae NAD nucleotidase reveals a novel enzymatic function of human CD73 related to NAD metabolism. The Biochemical journal *441*, 131–41.

Gebicke-Haerter, P. J., Christoffel, F., Timmer, J., Northoff, H., Berger, M. and Van Calker, D. (1996). Both adenosine A1- and A2-receptors are required to stimulate microglial proliferation. Neurochemistry International *29*, 37–42.

Geladopoulos, T. P., Sotiroudis, T. G. and Evangelopoulos, A. E. (1991). A malachite green colorimetric assay for protein phosphatase activity. Analytical Biochemistry *192*, 112–116.

Gijsbers, R., Ceulemans, H., Stalmans, W. and Bollen, M. (2001). Structural and catalytic similarities between nucleotide pyrophos-

phatases/phosphodiesterases and alkaline phosphatases. The Journal of Biological Chemistry *276*, 1361–1368.

Gilroy, D. W. (2004). Inflammatory resolution inflammation non-phlogistic NF-kB COX LOX COX-2 TGF cytokine lipoxin resolvin triHDHA DHA EPE apoptosis anticancer PPAR PPARg PGJ2 glucocorticoid annexin LXA4. Nature Rev Drug Disc *3*, 401.

Ginhoux, F., Greter, M., Leboeuf, M., Nandi, S., See, P., Gokhan, S., Mehler, M. F., Conway, S. J., Ng, L. G., Stanley, E. R., Samokhvalov, I. M. and Merad, M. (2010). Fate mapping analysis reveals that adult microglia derive from primitive macrophages. Science (New York, N.Y.) *330*, 841–5.

Guillemin, G. J. and Brew, B. J. (2004). Microglia, macrophages, perivascular macrophages, and pericytes: a review of function and identification. Journal of leukocyte biology *75*, 388–97.

Hanisch, U.-K. and Kettenmann, H. (2007). Microglia: active sensor and versatile effector cells in the normal and pathologic brain. Nature neuroscience *10*, 1387–94.

Hanisch, U. K., Prinz, M., Angstwurm, K., Häusler, K. G., Kann, O., Kettenmann, H. and Weber, J. R. (2001). The protein tyrosine kinase inhibitor AG126 prevents the massive microglial cytokine induction by pneumococcal cell walls. European Journal of Immunology *31*, 2104–2115.

Harrison, J. K., Jiang, Y., Chen, S., Xia, Y., Maciejewski, D., McNamara, R. K., Streit, W. J., Salafranca, M. N., Adhikari, S., Thompson, D. A., Botti, P., Bacon, K. B. and Feng, L. (1998). Role for neuronally derived fractalkine in mediating interactions between neurons and CX3CR1-expressing microglia. Proceedings of the National Academy of Sciences of the United States of America *95*, 10896–10901.

Haskó, G., Pacher, P., Deitch, E. A. and Vizi, E. S. (2007). Shaping of monocyte and macrophage function by adenosine receptors. Pharmacology & therapeutics *113*, 264–75.

Haskó, G., Pacher, P., Vizi, E. S. and Illes, P. (2005). Adenosine receptor signaling in the brain immune system. Trends in Pharmacological Sciences *26*, 511–516.

Häusler, K. G., Prinz, M., Nolte, C., Weber, J. R., Schumann, R. R., Kettenmann, H. and Hanisch, U.-K. (2002). Interferon-gamma differentially modulates the release of cytokines and chemokines in lipopolysaccharide- and pneumococcal cell wall-stimulated mouse microglia and macrophages. European Journal of Neuroscience *16*, 2113–2122.

Haynes, S. E., Hollopeter, G., Yang, G., Kurpius, D., Dailey, M. E., Gan, W.-B. and Julius, D. (2006). The P2Y12 receptor regulates microglial activation by extracellular nucleotides. Nature neuroscience *9*, 1512–9.

Hughes, M. M., Field, R. H., Perry, V. H., Murray, C. L. and Cunningham, C. (2010). Microglia in the degenerating brain are capable of phagocytosis of beads and of apoptotic cells, but do not efficiently remove PrPSc, even upon LPS stimulation. Glia *58*, 2017–30.

Inoue, K. (2008). Purinergic systems in microglia. Cellular and molecular life sciences : CMLS *65*, 3074–80.

Jacobson, K. A. and Gao, Z.-G. (2006). Adenosine receptors as therapeutic targets. Nature Reviews Drug Discovery *5*, 247–264.

Kettenmann, H., Hanisch, U.-K., Noda, M. and Verkhratsky, A. (2011). Physiology of microglia. Physiological reviews *91*, 461–553.

Kim, J. V. and Dustin, M. L. (2006). Innate response to focal necrotic injury inside the blood-brain barrier. The Journal of Immunology *177*, 5269–5277.

Koizumi, J., Yoshida, Y., Nakazawa, T. and Ohneda, G. (1986). Experimental studies of ischemic brain edema, I: a new experimental model of cerebral embolism in rats which recirculation can be introduced in the ischemic area. Japanese Journal of Stroke *8*, 1–8.

Koizumi, S., Shigemoto-Mogami, Y., Nasu-Tada, K., Shinozaki, Y., Ohsawa, K., Tsuda, M., Joshi, B. V., Jacobson, K. A., Kohsaka, S. and Inoue, K. (2007). UDP acting at P2Y6 receptors is a mediator of microglial phagocytosis. Nature *446*, 1091–5.

Krabbe, G., Matyash, V., Pannasch, U., Mamer, L., Boddeke, H. W. G. M. and Kettenmann, H. (2011). Activation of serotonin receptors promotes microglial injury-induced motility but attenuates phagocytic activity. Brain behavior and immunity *26*, 419–428.

Kukulski, F. and Komoszyński, M. (2003). Purification and characterization of NTPDase1 (ecto-apyrase) and NTPDase2 (ecto-ATPase) from porcine brain cortex synaptosomes. The Federation of European Biochemical Societies Journal *270*, 3447–3454.

Kukulski, F., Lévesque, S. A., Lavoie, E. G., Lecka, J., Bigonnesse, F., Knowles, A. F., Robson, S. C., Kirley, T. L., Sévigny, J. and Lavoie, E. G. (2005). Comparative hydrolysis of P2 receptor agonists by NTPDases 1, 2, 3 and 8. Purinergic Signalling *1*, 193–204.

Kukulski, F., Lévesque, S. A. and Sévigny, J. (2011). Impact of ectoenzymes on p2 and p1 receptor signaling. Advances in pharmacology (San Diego, Calif.) *61*, 263–99.

Kuypers, T. W., Eckmann, C. M., Weening, R. S. and Roos, D. (1989). A rapid turbidimetric assay of phagocytosis and serum opsonizing capacity. Journal of immunological methods *124*, 85–94.

Langer, D., Hammer, K., Koszalka, P., Schrader, J., Robson, S. and Zimmermann, H. (2008). Distribution of ectonucleotidases in the rodent brain revisited. Cell and Tissue Research *334*, 199–217.

Leonard, E. J., Skeel, A., Chiang, P. K. and Cantoni, G. L. (1978). The action of the adenosylhomocysteine hydrolase inhibitor, 3-deazaadenosine, on phagocytic function of mouse macrophages and human monocytes. Biochemical and biophysical research communications *84*, 102–9.

Liu, G.-D., Ding, J.-Q., Xiao, Q. and Chen, S.-D. (2009). P2Y6 receptor and immunoinflammation. Neuroscience bulletin *25*, 161–4.

Liu, Y., Walter, S., Stagi, M., Cherny, D., Letiembre, M., Schulz-Schaeffer, W., Heine, H., Penke, B., Neumann, H. and Fassbender, K. (2005). LPS receptor (CD14): a receptor for phagocytosis of Alzheimer's amyloid peptide. Brain: A journal of neurology *128*, 1778–1789.

Magnus, T., Chan, A., Grauer, O., Toyka, K. V. and Gold, R. (2001). Microglial phagocytosis of apoptotic inflammatory T cells leads to down-regulation of microglial immune activation. The Journal of Immunology *167*, 5004–10.

Mallat, M., Marín-Teva, J. L. and Chéret, C. (2005). Phagocytosis in the developing CNS: more than clearing the corpses. Current opinion in neurobiology *15*, 101–7.

Markovic, D. S., Glass, R., Synowitz, M., Rooijen, N. V. and Kettenmann, H. (2005). Microglia stimulate the invasiveness of glioma cells by increasing the activity of metalloprotease-2. Journal of neuropathology and experimental neurology *64*, 754–762.

Martin, E. and Bhakdi, S. (1991). Quantitative analysis of opsonophagocytosis and of killing of Candida albicans by human peripheral blood leukocytes by using flow cytometry. Journal of clinical microbiology *29*, 2013–23.

Matzinger, P. (2007). Friendly and dangerous signals: is the tissue in control? Nature Immunology *8*, 11–13.

Millán, J. L. (2006). Alkaline Phosphatases. Purinergic Signalling *2*, 335–341.

Morgan, D., Gordon, M. N., Tan, J., Wilcock, D. and Rojiani, A. M. (2005). Dynamic complexity of the microglial activation response in transgenic models of amyloid deposition: implications for Alzheimer therapeutics. Journal of neuropathology and experimental neurology *64*, 743–53.

Mori, S. and Nagano, M. (1985). Electron-microscopic cytochemistry of alkaline-phosphatase activity in endothelium, pericytes and oligodendrocytes in the rat brain. Histochemie *82*, 225–231.

Murabe, Y. and Sano, Y. (1982). Morphological studies on neuroglia. VI. Postnatal development of microglial cells. Cell and tissue research *225*, 469–85.

Nimmerjahn, A., Kirchhoff, F. and Helmchen, F. (2005). Resting microglial cells are highly dynamic surveillants of brain parenchyma in vivo. Science (New York, N.Y.) *308*, 1314–8.

Ogata, T. and Schubert, P. (1996). Programmed cell death in rat microglia is controlled by extracellular adenosine. Neuroscience Letters *218*, 91–94.

Parkinson, F. E., Damaraju, V. L., Graham, K., Yao, S. Y. M., Baldwin, S. A., Cass, C. E. and Young, J. D. (2011). Molecular biology of nucleoside

transporters and their distributions and functions in the brain. Current Topics in Medicinal Chemistry *11*, 948–972.

Parkinson, F. E., Xiong, W. and Zamzow, C. R. (2005). Astrocytes and neurons: different roles in regulating adenosine levels. Neurological Research *27*, 153–160.

Pastor-Anglada, M., Felipe, A., Casado, F. J., Del Santo, B., Mata, J. F. and Valdés, R. (1998). Nucleoside transporters and liver cell growth. Biochemistry and cell biology Biochimie et biologie cellulaire *76*, 771–777.

Perry, V. H., Nicoll, J. A. R. and Holmes, C. (2010). Microglia in neurodegenerative disease. Nature reviews. Neurology *6*, 193–201.

Peterson, P. K., Verhoef, J., Schmeling, D. and Quie, P. G. (1977). Kinetics of phagocytosis and bacterial killing by human polymorphonuclear leukocytes and monocytes. The Journal of infectious diseases *136*, 502–9.

Pexa, A. and Deussen, A. (2005). Modulation of ecto-5'-nucleotidase by phospholipids in human umbilical vein endothelial cells (HUVEC). Naunyn-Schmiedeberg's archives of pharmacology *372*, 131–8.

Prinz, M., Kann, O., Draheim, H. J., Schumann, R. R., Kettenmann, H., Weber, J. R. and Hanisch, U. K. (1999). Microglial activation by components of gram-positive and -negative bacteria: distinct and common routes to the induction of ion channels and cytokines. Journal of neuropathology and experimental neurology *58*, 1078–1089.

Ransohoff, R. M. and Perry, V. H. (2009). Microglial physiology: unique stimuli, specialized responses. Annual review of immunology *27*, 119–45.

Robson, S. C., Sévigny, J. and Zimmermann, H. (2006). The E-NTPDase family of ectonucleotidases: Structure function relationships and pathophysiological significance. Purinergic signalling *2*, 409–30.

Salmon, J. E., Brogle, N., Brownlie, C., Edberg, J. C., Kimberly, R. P., Chen, B. X. and Erlanger, B. F. (1993). Human mononuclear phagocytes express adenosine A1 receptors. A novel mechanism for differential regulation of Fc gamma receptor function. Journal of immunology (Baltimore, Md. : 1950) *151*, 2775–85.

Saura, J. (2007). Microglial cells in astroglial cultures: a cautionary note. Journal of Neuroinflammation *4*, 26.

Schenk, D., Barbour, R., Dunn, W., Gordon, G., Grajeda, H., Guido, T., Hu, K., Huang, J., Johnson-Wood, K., Khan, K., Kholodenko, D., Lee, M., Liao, Z., Lieberburg, I., Motter, R., Mutter, L., Soriano, F., Shopp, G., Vasquez, N., Vandevert, C., Walker, S., Wogulis, M., Yednock, T., Games, D. and Seubert, P. (1999). Immunization with amyloid-beta attenuates Alzheimer-disease-like pathology in the PDAPP mouse. Nature *400*, 173–7.

Schilling, M., Besselmann, M., Müller, M., Strecker, J. K., Ringelstein, E. B. and Kiefer, R. (2005). Predominant phagocytic activity of resident microglia over hematogenous macrophages following transient focal cerebral ischemia: an investigation using green fluorescent protein transgenic bone marrow chimeric mice. Experimental neurology *196*, 290–7.

Schipke, C. G., Haas, B. and Kettenmann, H. (2008). Astrocytes discriminate and selectively respond to the activity of a subpopulation of neurons within the barrel cortex. Cerebral Cortex *18*, 2450–2459.

Si, Q. S., Nakamura, Y., Schubert, P., Rudolphi, K. and Kataoka, K. (1996). Adenosine and propentofylline inhibit the proliferation of cultured microglial cells. Experimental Neurology *137*, 345–349.

Simard, A. R., Soulet, D., Gowing, G., Julien, J.-P. and Rivest, S. (2006). Bone marrow-derived microglia play a critical role in restricting senile plaque formation in Alzheimer's disease. Neuron *49*, 489–502.

Sowa, N. A., Vadakkan, K. I. and Zylka, M. J. (2009). Recombinant mouse PAP has pH-dependent ectonucleotidase activity and acts through A1-adenosine receptors to mediate antinociception. PLoS ONE *4*.

Sperlágh, B. and Illes, P. (2007). Purinergic modulation of microglial cell activation. Purinergic signalling *3*, 117–27.

Stefan, C., Jansen, S. and Bollen, M. (2005). NPP-type ectophosphodiesterases: unity in diversity. Trends in Biochemical Sciences *30*, 542–550.

Streit, W. J., Walter, S. A. and Pennell, N. A. (1999). Reactive microgliosis. Progress in Neurobiology *57*, 563–581.

Vivian, J. P., Riedmaier, P., Ge, H., Le Nours, J., Sansom, F. M., Wilce, M. C. J., Byres, E., Dias, M., Schmidberger, J. W., Cowan, P. J., D'Apice, A. J. F., Hartland, E. L., Rossjohn, J. and Beddoe, T. (2010). Crystal structure of a Legionella pneumophila ecto -triphosphate diphosphohydrolase, a structural and functional homolog of the eukaryotic NTPDases. Structure London England 1993 *18*, 228–238.

Vollmayer, P., Clair, T., Goding, J. W., Sano, K., Servos, J. and Zimmermann, H. (2003). Hydrolysis of diadenosine polyphosphates by nucleotide pyrophosphatases/phosphodiesterases. The Federation of European Biochemical Societies Journal *270*, 2971–2978.

von Zahn, J., Möller, T., Kettenmann, H. and Nolte, C. (1997). Microglial phagocytosis is modulated by pro- and anti-inflammatory cytokines. Neuroreport *8*, 3851–6.

Vorbrodt, A. W., Lossinsky, A. S. and Wisniewski, H. M. (1982). Cytochemical localization of ouabain-sensitive, K+-dependent p-nitro-phenylphosphatase (transport ATPase) in the mouse central and peripheral nervous systems. Brain Research *243*, 225–234.

Vorbrodt, A. W., Lossinsky, A. S. and Wisniewski, H. M. (1986). Localization of alkaline phosphatase activity in endothelia of developing and mature mouse blood-brain barrier. Developmental Neuroscience *8*, 1–13.

Wake, H., Moorhouse, A. J., Jinno, S., Kohsaka, S. and Nabekura, J. (2009). Resting microglia directly monitor the functional state of synapses in vivo and determine the fate of ischemic terminals. The Journal of neuroscience : the official journal of the Society for Neuroscience *29*, 3974–80.

Ward, S. A., Ransom, P. A., Booth, P. L. and Thomas, W. E. (1991). Characterization of ramified microglia in tissue culture: pinocytosis and motility. Journal of neuroscience research *29*, 13–28.

Yegutkin, G. G. (2008). Nucleotide- and nucleoside-converting ectoenzymes: Important modulators of purinergic signalling cascade. Biochimica et Biophysica Acta *1783*, 673–694.

Zimmermann, H. (1992). 5'-Nucleotidase: molecular structure and functional aspects. The Biochemical journal *285 (Pt 2*, 345–65.

Zimmermann, H. (2001). Ectonucleotidases: Some recent developments and a note on nomenclature. Drug Development Research *52*, 44–56.